

This work was written as part of one of the author's official duties as an Employee of the United States Government and is therefore a work of the United States Government. In accordance with 17 U.S.C. 105, no copyright protection is available for such works under U.S. Law.

Public Domain Mark 1.0

<https://creativecommons.org/publicdomain/mark/1.0/>

Access to this work was provided by the University of Maryland, Baltimore County (UMBC) ScholarWorks@UMBC digital repository on the Maryland Shared Open Access (MD-SOAR) platform.

Please provide feedback

Please support the ScholarWorks@UMBC repository by emailing scholarworks-group@umbc.edu and telling us what having access to this work means to you and why it's important to you. Thank you.

Calibration and Validation for the Surface Biology and Geology (SBG) Mission Concept: Recommendations for a Multi-Sensor System for Imaging Spectroscopy and Thermal Imagery

Kevin R. Turpie^{1,6}, Kimberly A. Casey², Christopher J. Crawford³, Liane S. Guild⁴,
Hugh Kieffer⁵, Guoqing (Gary) Lin⁶, Raymond Kokaly⁷, Alok K. Shrestha⁴, Cody
Anderson³, Shankar N. Ramasari Chandra^{3,8}, Robert Green⁹, Simon Hook⁹, Constantine
Lukashin¹⁰, Kurt Thome⁶

¹ University of Maryland, Baltimore County.

² US Geological Survey, Reston Virginia.

³ US Geological Survey, Earth Resources Observation and Science Center

⁴ NASA Ames Research Center.

⁵ Celestial Reasonings, Genoa Nevada.

⁶ NASA Goddard Space Flight Center.

⁷ US Geological Survey, Denver Colorado.

⁸ KBR Incorporated.

⁹ California Institute of Technology.

¹⁰ NASA Langley Research Center.

Corresponding author: K.R. Turpie (kturpie@umbc.edu)

Key Points:

- Overviews cal/val ideas recommended for the SBG mission, with some consideration for collaborating with multiple contemporary missions.
- Looks at approaches to inter-calibration of multiple Earth orbiting sensors.
- Surveys what cal/val resources and techniques are currently available or may be available to the SBG mission later in this decade.

Abstract

The primary objective of the NASA Surface Biology and Geology (SBG) mission is to measure biological, physical, chemical, and mineralogical features of the Earth's surface, realizing a key conceptual component of the envisioned NASA Earth System Observatory (ESO). SBG is planned to launch as a two-platform mission in the late 2020s, the first of the ESO satellites. Targeted science and applications objectives based on observations of the Earth's surface biology and geology helped to define the mission architecture and instrument capabilities for the SBG mission concept. These objectives further drove the need for enabling change detection and trending of surface biological and geological features. These needs implied fundamental

This article has been accepted for publication and undergone full peer review but has not been through the copyediting, typesetting, pagination and proofreading process, which may lead to differences between this version and the [Version of Record](#). Please cite this article as [doi: 10.1029/2023JG007452](#).

This article is protected by copyright. All rights reserved.

calibration goals to achieve the necessary science data quality characteristics. To meet those goals, calibration and validation pre-launch and on-orbit methods formed a basis of the calibration and validation concept, including the combined use of on-board references, vicarious techniques, and routine lunar imaging. International collaboration with space agencies in other countries, an important feature of the recommended SBG mission architecture, uncovered and emphasized the need for inter-calibration techniques that underscored the importance of collaborative instrument characterization data sharing and the use of common calibration references that are International System of Units (SI) traceable in pre-launch and post-launch on orbit calibration mission phases. International collaboration through the use of terrestrial and aquatic networks on six continents for vicarious calibration and validation activities will further assure necessary science data quality while in orbit.

1 Introduction

The National Aeronautics and Space Administration (NASA) Surface Biology and Geology (SBG) Designated Observable (DO) science and application objectives, as outlined in the 2017 National Academies of Science, Engineering and Medicine Committee on Earth Science and Application from Space (ESAS) Decadal Survey report (National Academies of Sciences, Engineering, and Medicine, 2018), were used to conceptualize the SBG mission architecture. These objectives included global observation, change detection, and trending of terrestrial and aquatic surface ecosystems, hydrology, geology and their effect on weather and climate. Measurements must be able to detect seasonal and long-term changes for addressing dynamics of the Earth System and Essential Climate Variables (ECV) to advance the investigations of climatic change and impacts. To address the global scope of the science, SBG must provide global coverage of land, island, and coastal and inland waters. These objectives and observations were described in the Science and Applications Traceability Matrix (SATM) described by Stavros et al. (2022). This supplied the SBG project with its research and applications objectives.

These objectives drove choices of mission architecture, instrument characteristics and performance and further established fundamental calibration and validation goals needed to achieve the implied science data quality characteristics (Stavros et al., 2022), which are summarized in Table 1. The implications also led to mission characteristics provided in Table 2. To acquire Earth observations globally with sufficient spatial, spectral and temporal resolutions and ranges to meet these mission characteristics, NASA plans to use two separate free-flying platforms, each in low-Earth, polar, sun-synchronous orbits. These orbits must provide repeatable Sun-sensor geometry for consistency in retrievals and for calibration and validation, and provide for consistent global coverage. One satellite would be in a descending morning orbit similar to satellites in the Landsat series and support a imaging spectrometer covering wavelengths from ~ 0.4 to $2.5 \mu\text{m}$ (i.e., visible-to-shortwave infrared or VSWIR) and another satellite in descending afternoon orbit carrying a multi-band, thermal infrared (TIR) imager. The target launch date of the two-platform mission is early 2028, making these the first of the Earth System Observatory (ESO) satellites planned by NASA to fly.

In addition, in order to improve temporal sampling, the SBG mission architecture was extended to include potential cooperation with agencies of other nations. Two independent, polar-orbiting VSWIR imaging spectrometers from the European Union and European Space Agency (ESA) Copernicus Hyperspectral Imaging Mission for the Environment (CHIME) (Celesti et al., 2022)

would potentially complement the SBG VSWIR imaging spectrometer. In addition, two polar-orbiting thermal imagers from ESA's Copernicus Land Surface Temperature Monitoring (LSTM; <https://www.eoportal.org/satellite-missions/lstm>) and the future polar-orbiting thermal imager of the Thermal infraRed Imaging Satellite for High-resolution Natural resource Assessment (TRISHNA; <https://trishna.cnes.fr/en/trishna-0>) planned by National Centre for Space Studies (CNES) and Indian Space Research Organization (ISRO), would likewise complement the SBG thermal imager. The desired coordination of observations from these multiple platforms implied the need for inter-calibration techniques, which likewise underscored the further need for collaborative sharing of instrument characterization data, the use of common reference data, and the implementation of data harmonization.

The SBG mission architecture and its intended science and application objectives naturally led to the decisions for support of pre-launch and on-orbit calibration elements. For instance, inter-consistency of observations over time of the same instrument for change detection and global mosaicking implied accuracy goals for in-flight calibration monitoring and the need for on-board references, lunar calibration and vicarious calibration (discussed in Section 5). The SBG project could not determine well-defined accuracy requirements for data products used to meet the science and applications objectives outlined in Stavos et al. (2022). However, good calibration and validation, is understood to be an essential tool to ensure measurement quality will be sufficient in terms of radiometric accuracy, data product quality and temporal stability (Masek et al., 2020; Xiong et al., 2020). The purpose of this paper is to survey both general and specific concepts needed to be realized to provide adequate capacity for calibration and validation in light of SBG science and applications objectives.

The SBG project initially chartered the Calibration and Validation Working Group (CVWG) to scope, establish, and recommend calibration and validation strategies for SBG observations with input from the global imaging spectroscopy community. The CVWG is led by two co-authors of this paper (Turpie & Kokaly) and includes all the other co-authors along with over 100 experts from dozens of remote sensing and metrology organizations worldwide. Initially, the CVWG identified a set of high-level calibration and validation schemes that would constitute plans for pre-launch and post-launch calibration of SBG VSWIR and TIR instruments and validation of calibrated data products derived from remote measurements. This included scoping pre-launch instrument characterization activities, defining potential objectives for vicarious and on-orbit calibration, and describing validation strategies for mission data products. The CVWG also considered the need to identify calibration reference sites and measurements to satisfy post-launch calibration and validation objectives. The CVWG also evaluated basic needs for data product validation from the calibrated measurements above the top-of-atmosphere (TOA) based on a broad concept of what data products might be provided. This involved the identification of external *in situ* measurement resources and organizations through which appropriate vicarious calibration and validation activities could be conducted. An initial inventory of these potential resources was created to help scope the SBG validation concept and determine what may be available for vicarious calibration.

Further work by the CVWG is expected to continue through the mission development life cycle, especially closer to launch to reduce the risk that needed resources are not available during flight and allow for further development of data product quality requirements. This paper provides an overview of the SBG mission calibration concept with consideration for inter-calibration needs

among collaborating Earth observation missions on data product harmonization agreements and provides numerous recommendations by the SBG CVWG. In Section 2, we discuss recommendations toward cross-mission commonality, including spectroscopy, remote sensing, scientific, engineering and calibration terms, data product harmonization, and reference data set management. In Section 3, we consider the mission essential pre-launch instrument characterization and calibration steps. Section 4 covers orbital planning and the calibration opportunities afforded by coordination with other Earth observation missions. Multiple scenarios are presented regarding near-simultaneous mission and scene acquisition overlap. Calibration and monitoring are presented in Section 5. We discuss mission onset or commissioning and long-term monitoring recommendations via standard references of the Earth, Moon and Sun calibration and radiometric, thermal, and geometric targets. This includes some description of major surface resources that are likely to be supported by SBG launch. We summarize SBG relevant high-level calibration and validation concepts, as well as overall project recommendations outlined in the paper in the final section. Appendix A lists the acronyms used in this paper.

Further development of SBG calibration and validation strategies will come with the formulation of the SBG mission. Fortunately, with close to 40 years of experience with airborne imaging spectrometers (e.g., Airborne Imaging Spectrometer (AIS), Vane et al., 1984; Airborne Visible / InfraRed Imaging Spectrometer (AVIRIS)-Classic, Green et al, 1998; AVIRIS-Next Generation, Chapman et al., 2019; and HyMap, Cocks et al, 1998) there is broadening experience with such instruments and data. Many recent imaging spectrometer missions are currently operating in space, including Compact High Resolution Imaging Spectrometer (CHRIS) on Project for On-Board Autonomy (PROBA)-1 (Barnsley et al., 2004), the Chinese Tiangong-1 (Li et al., 2016), the Italian PRecursoRe IperSpettrale della Missione Applicativa (PRISMA) mission (Pignatti et al., 2013), Japan's Hyperspectral Imager Suite (HISUI) (Iwasaki et al., 2011), the German DLR, (Deutsches Zentrum für Luft- und Raumfahrt) Earth Sensing Imaging Spectrometer (DEISIS) sensor (Krutz et al., 2019), as well as new missions such as the German Environmental Mapping and Analysis Program (EnMAP) (Alonso et al., 2019) launched April 2022, NASA's Earth Surface Mineral Dust Source Investigation (EMIT) launched July 2022 (Green et al., 2020), the Israeli/Italian Space-borne Hyperspectral Applicative Land and Ocean Mission (SHALOM) concept (Feingersh and Ben-Dor, 2015), and European Space Agency (ESA)'s FLuorescence EXplorer (FLEX) mission (Coppo et al., 2017).

Further, synergies with other NASA hyperspectral satellite missions, namely the Plankton, Aerosol, Cloud, ocean Ecosystem (PACE) (Werdell et al., 2019), which is planned to be launched early in 2024, and the Geostationary Littoral Imaging and Monitoring Radiometer (GLIMR) (Salisbury, 2022), which is planned to launch in 2026, will enable calibration and validation concept testing and implementation for aquatic acquisitions prior to SBG launch. SBG will collaborate with the other missions supported by the USA for algorithm development and evaluation and regarding calibration and validation resources and efforts. To help facilitate such collaboration the Aquatic Cross-Mission Exchange (ACME) was created to provide a forum for discussions between SBG, PACE and GLIMR. Of particular importance will be the sharing of *in situ* data from a jointly established infrastructure of surface calibration and validation measurement network, starting with what was described in Section 5. Because of the success

and future potential of the ACME, the Terrestrial Cross-Mission Exchange (TCME) was later created for collaboration between SBG, EMIT and Landsat and possibly other missions.

Table 1. *SBG Research and Applications Objectives and Mission and Cal/Val Implications*

Research and Application Objectives	Implications for Mission and Cal/Val Requirements
<p>TYPES OF OBSERVATIONS: Measure ecosystem function, plant functional diversity, aquatic ecosystem characteristics, coastal benthic cover, soil and mineral properties, ice and snow conditions across complex terrains. Measurements will also allow observation of events such as oil spills, volcanic eruptions, and wildfires.</p>	<p>Objectives require mission characteristics listed in Table 2 for a VSWIR spectroscopy thermal imagery mission.</p> <p>Measurements, especially dark targets such as aquatic ones, will require accurate calibration and prelaunch characterization.</p>
<p>SPATIAL REQUIREMENTS: Coverage must be global with spatial resolution to capture spatial variability of key surface features related to biological and geological features.</p>	<p>Spatial requirements are given in Table 2. Such resolution implied highly accurate geometric calibration and prelaunch spatial characterization.</p> <p>Geometric consistency is provided by orbital parameters in Table 2.</p> <p>Global coverage implies stable instrument calibration and good prelaunch characterization to reduce overlap artifacts in mosaics. Stable instrument calibration suggests in-flight monitoring and calibration correction.</p>
<p>TEMPORAL REQUIREMENTS: Observations will be made at sub-seasonal and yearly time scales and sufficient detail to quantify variation and ability to observe rapid or transient changes related to Earth system events such as fires, landslides, volcanic activity and anthropogenic incidents.</p> <p>To achieve optimal temporal resolution, SBG intends to harmonize data with collaborating international missions to maximize temporal sampling.</p>	<p>The system's orbit provide consistent sun-sensor geometry for observation consistency in retrievals and for calibration and validation, and provide for global coverage, as above (polar orbit). This leads to orbital parameters given in Table 2.</p> <p>Change, cycle and trend detection implies stable calibration via on-orbit commissioning, in-flight monitoring and calibration corrections. The latter suggests elements such as lunar calibration, solar calibration or on-board references, including a black body for TIR or lamps for VSWIR.</p> <p>Data harmonization implies inter-calibration, inter-validation, share methodologies and references.</p>

Table 2. *SBG Mission Characteristics and Instrument Specifications*

	Mission Characteristic	VSWIR Imaging Spectrometer	Thermal Imager
GENERAL	Architecture Description	One satellite with a VSWIR imaging spectrometer and one satellite with a TIR imager	
	Orbit Type	LEO Polar Sunsynchronous, LTDN 1030-1130	LEO Polar Sunsynchronous, LTDN 1230 \pm 5 min
	Altitude	619 km	666 km
	Prospective Launch Date	NET 2028 Q1	NET 2028 Q1
	Tilt	3-5° fixed along scan tilt (for glint avoidance)	None
TEMPORAL	Observation Frequency	≤ 16 days (5-8 days w/ CHIME)	≤ 3 days (≤ 2 days w/ LSTM & TRISHNA)
	Resolvable Time Scales	Seasonal to Decadal	Seasonal to Decadal
SPATIAL	Coverage	Global land, coastal, island & inland waters	Global land, coastal, island & inland waters
	Events Targeting	Significant phenomena and cal/val activities	Significant phenomena and cal/val activities
	Swath width	185 km	930 km
	Ground Sample Distance	30 m (1km over open ocean)	60 m (1km over open ocean)
SPECTRAL	Spectral Range	380-2500 nm (can reach 320 nm)	3-12 μ m (multiple bands)
	Spectral Resolution	8-12 nm	TBD
	Spectral Sampling	10 nm	TBD
	# Bands	>210	5-8
RADIOMETRIC	Performance	VNIR (0.5-1.0 μ m): SNR > 400 @ 25% reflectance SWIR (1.6-2.2 μ m): SNR > 250, @ 25% reflectance	TIR (8-12 μ m): 0.2°K NeDT @ 275°K, 200-500°K MIR (3-5 μ m): 0.3°K NeDT @ 750°K, 400-1200°K
	Number of Bits	≥ 14	≥ 14

2 Recommendations Towards Cross-Mission Commonality

2.1 Common Metrological Language and Terms for Spaceborne Remote Sensing Techniques

The SBG CVWG recommended consistent use of commonly used metrological and radiometric terminology specific to imaging spectroscopy and thermal imaging across SBG and collaborating missions. Where possible, such terminology should be derived from international standards (e.g., BIPM et al., 2008; Ferrero, 2009; Nicodemus et al., 1977; Schaepman-Strub et al., 2006). This metrological lexicon should include, but not be limited to terms such as ‘calibration,’ ‘validation,’ ‘uncertainty,’ ‘accuracy,’ ‘precision,’ and ‘reflectance.’ Of particular interest for common terms and definitions for the imaging spectroscopy community is the Institute of Electrical and Electronics Engineers (IEEE) P4001 working group effort, which is ongoing, for setting hyperspectral standards for VSWIR imaging spectrometers (Durell, 2019; <https://standards.ieee.org/project/4001.html>).

For the purposes of this paper, the SBG CVWG defines and distinguishes ‘calibration’ and ‘validation’ as unique mission components as outlined by the Committee on Earth Observation

Satellites (CEOS) Working Group on Calibration and Validation (WGCV). The process of ‘calibration’ is quantitatively defining a system’s response to known and controlled signal inputs (CEOS <https://ceos.org/ourwork/workinggroups/wgcv/>). For SBG the measured quantities to be related to sensor responses will be radiance and brightness temperature. Among the factors that affect the magnitude of these quantities, are instrument response and stability, characteristics of the surface (e.g., chemical composition, biological composition and activity, and physical structure that affect optical and radiative properties and measures such as surface reflectance and emissivity), state of the atmosphere (e.g., concentration and sizes of gasses and particulates), and other factors that may vary over time and by geographic location (e.g., solar irradiance, view and illumination geometry, surface topography). In this paper we touch on all these factors whether they are derived products to validate, are inputs to models, or are reference datasets needed to calibrate SBG sensors.

In the context of this paper, we take calibration simply as the act of making a one-to-one association of a physical measurement scale to an instrument response. Further, we must also understand and characterize how the instrument samples these scales and the expected uncertainty of each sample given instrument characteristics. For the SBG mission, three main types of physical measurement scales are of import:

1. Radiometric scale, which places a scale in physical units on instrument response in the form of a digital readout. The scale is in units of radiance in the VSWIR measurements. Radiometric resolution is determined mostly by the noise level as function of radiance, the digital sampling of the radiometric scale and followed possibly by other factors such as temperature.
2. Spectral scale, which assigns wavelength positions to spectral channels and defines the bandpasses of the spectral channels. This includes response as a function of wavelength, which is commonly modeled with gaussian or similar mathematical function for imaging spectrometers and is defined as the spectral response function for broadband sensors.
3. Geometric scale, a multi-dimensional metric, which ultimately facilitates geolocation, i.e., placing spectra on a spatial grid, determines sun-surface-sensor geometry. In this paper, we include the spatial response and sampling characteristics of the instrument with the geometric scale.

Calibration is ‘absolute’ if it can associate a measurement scale for the instrument response that is traceable to national or international standards with an instrument system response. A calibration is ‘relative’ if it adjusts a previously mapped scale relative to match some other presumably more accurate scale. This could involve any affine transformation, including application of a scale adjustment factor or offset. Relative calibration usually involves characterizing differences, either between two instruments or with the same instrument with changing conditions or with time. For adjustments based on comparisons over time, Müller (2014) gave the term re-calibration. In this latter case of relative calibration, removal of drift in instrument response over time is made by trending or monitoring instrument behavior. For clarity, the SBG CVWG refers to this as a ‘time-dependent relative calibration’.

Vicarious calibration is any radiometric calibration method that uses well-characterized, stable and uniform targets on the Earth’s surface as a reference. This includes pseudo-invariant sites that are actively instrumented *in situ* (e.g., the Radiometric Calibration Network, RadCalNet;

Bouvet et al., 2019) and sites that are episodically measured during field campaigns, for example, during a commissioning phase or later evaluation period (Storch et al., 2014). The modifier ‘vicarious’ is used because a spaceborne instrument is being indirectly calibrated using instruments on the ground, i.e., transferring radiometric scales from instruments on Earth to a spaceborne instrument using the Earth’s surface as an intermediate reference. All vicarious calibration for Earth observing satellites must contend with the Earth’s atmosphere to some degree, especially targets that have relatively low reflectance signatures (e.g., deep, clear water).

The terms inter-calibration and cross-calibration appear in the literature as interchangeable, however, we will only use the term inter-calibration to establish absolute calibration scales on two or more instruments so that they produce measurements that agree within a known uncertainty. This usually involves use of a common, well known reference by all instruments being inter-calibrated. This could include either the transfer of a scale from another more accurately calibrated instrument using near identical observations (i.e., close in time and geometry) or a well-characterized source.

The measurements of two instruments can be compared for inter-consistency. The general use of statistical comparisons of Earth observations between instruments to determine inter-consistency alone cannot facilitate inter-calibration unless one instrument can serve as a reference or the targets are well known. Forcing inter-consistency by relatively adjusting one or more instruments based on an inter-comparison to a single reference instrument (or an average of all instruments) or well-known target yields no better accuracy than that of the chosen reference. Unless a reference instrument provides accurate, International System of Units (SI) traceable measurements, this approach is of limited use for calibration purposes. However, simple inter-comparison and adjustment for inter-consistency can help with objectives such as seamless mosaicking of satellite imagery.

Finally, CEOS defines validation as

“... the process of assessing, by independent means, the quality of the data products derived from those system outputs” (<https://ceos.org/ourwork/workinggroups/wgcv/>).

In this sense, we consider validation as the comparison of independent data or measurements against remote sensing model or algorithm predictions to determine the accuracy of those predictions. With regard to independence, it is important to note, that as a rule, the exact same data or measurements used for validation must not also be used for training or calibration.

2.2 Data Product Harmonization

In the context of the SBG concept, an objective of calibration and validation in data product harmonization is to produce inter-consistent observations of the Earth’s surface. To facilitate this, the SBG CVWG recommended that participating agencies keep as much information and steps in common as possible for a suite of standard data products across missions. This starts with sharing pre-launch characterization reference sources and techniques; exchanging instrument characterization data; sharing field observation data to execute validation and potential inter-calibration; establishing common standardized reference datasets and models; and identifying standard data products and algorithms. SBG CVWG also recommended that the

collaborating organizations should have advanced discussions and agreements regarding communication, work-flows, and conflict resolution necessary for effective collaboration towards these common resources. Ideally, resulting approaches or solutions should be reviewed by an external internationally recognized organization, such as the CEOS WGCV or similar international body.

In addition to harmonization, facilitating data product interoperability may be useful for collaborative work across agencies using common tools. The SBG CVWG recommended that these tools include transformation of high-level data products onto common spatial grids. The collaborating teams should also agree on an interoperable format and metadata. This would entail identifying and establishing a data product format including metadata that would support interoperability of all global imaging spectroscopy and multispectral TIR measurements across sensor data products, organizations, and analysis tools. The SBG CVWG recommended use of International Organization for Standardization (ISO) data standard or CEOS protocols for development of Analysis Ready Data (ARD) (Dwyer et al., 2018 and see <http://ceos.org/ard/>). Wherever possible, the collaborating teams should use standard, open source algorithms, ideally following NASA's Open Source Science Initiative (<https://science.nasa.gov/open-science-overview>), including algorithms that produce at-sensor measurement and surface radiometry and geometry. The collaborating teams should work to standardize and control the quality of reference datasets. This includes determining what, if any, reference data sets (as described earlier) should be standardized and quality controlled across collaborating missions and whether an international standard protocol, format, and metadata should be used.

The data product harmonization details are of course complex. Collaborating organizations and space agencies often establish data agreements and corresponding government licenses to share data as controlled by law. This entails first determining what restrictions, if any, prevent or delay the timely release of instrument characterization or calibration data. Similarly, this also applies to calibration and validation data from collaborating agency surface measurement networks or from spaceborne or airborne missions. Steps must also be taken to establish the appropriate agreements for data access and use by data product end users to ensure that independent community assessment of data quality is also possible.

It is also recommended that an analysis infrastructure be established. This involves developing computational infrastructure and analysis tools (e.g., identified through Cal/Val strategies or protocols) for comparing SBG imaging spectroscopy or thermal infrared imagery with data sets from other surface, airborne, or spaceborne sensors, as provided by collaborating agencies. Some part of this infrastructure may be developed by the community, while another portion could be developed by the collaborating missions. This would further data product interoperability and consistency of analysis. It would also further support the production of ARD, the requirement of which is currently being developed by the CEOS. NASA's Open Source Science Initiative aligns with ARD and implements policies on software, publication, and data enabling integration and improved data management, access, computing, analytics, and

scientific collaboration. Such effort would facilitate capacity building, partner engagement, and incentives to help accelerate scientific discovery through open science.

2.3 Reference Data Set Management

Instrument calibration data are applied in the processing of raw telemetry to at-sensor imagery with geophysical units and geolocation. The processing and the generation of downstream science data products, including surface radiometry and temperature, critically depend on reference data sets and standard models. To facilitate data harmonization, it is recommended that these reference data sets and standard models be standardized and version controlled, ideally across all space agencies collaborating with the SBG mission. If data products are harmonized across sensors from multiple collaborating space agencies, those organizations must agree on the metadata, format and stewardship of all of such data sets. In addition, reference data archiving, distribution, and configuration control should be planned, especially for data sets that change frequently. This also likely necessitates advanced agreements and/or understandings and possibly shared agency responsibilities. Listed in Table 3 are some key examples.

Table 3. *Examples Reference Datasets and Models[†]*

Reference Data Set or Model	Purpose
Star catalog and planetary ephemeris data	Geo Cal
Leap second and polar wander that includes (UT1-UTC)	Geo Cal
Ground Control Point (GCP) database or Global Reference Image (GRI)	Geo Cal
Time-dependent calibration adjustments	Rad Cal
Lunar irradiance model (e.g., ROLO, GIRO or LIME)*	Rad Cal
Solar irradiance spectrum*	Rad Cal, Reflectance
Instrument char. data (e.g., radiometric, spectral and polarization responses)	Rad Cal, Reflectance
Vicarious calibration adjustments	Reflectance
Spectral transmission of absorbing gasses (e.g., H ₂ O, O ₃ , NO ₂)*	Reflectance
Meteorological data (e.g., wind, relative humidity, pressure and temperature)	Reflectance
Aerosol models	Reflectance
BRDF models of vicarious calibration sites	Reflectance
Digital Elevation Model (DEM) and Earth Gravitational Model (e.g., EGM96)	Geo Cal
Inland water body masks or land/water masks	Reflectance
Land/sea masks	Reflectance
Bathymetry	Reflectance, Science Data
Global shoreline vector data set	Science Data
Sea surface temperature climatology	Science Data
Geological and pedological map	Science Data
Spectral libraries*	Science Data

* Must be taken with respect to the spectral response of the instruments.

[†] In Table 3, note references support geometric calibration (**Geo Cal**), radiometric calibration (**Rad Cal**), surface reflectance (**Reflectance**) or the generation of certain science data products (**Science Data**), with some supporting more than one.

As mentioned, these reference data sets are important to the generation and validation of mission data products. Ephemeris and leap second data are important to accurately determine the position of the spacecraft, which is used in geolocation and estimating solar irradiance for onboard

calibration using the Sun. Instrument characterization data play a role in processing calibrated TOA measurements and also for surface measurements, specifically because they can provide key information for atmospheric correction. A standard solar irradiance data set is key to generating reflectance values and is also essential to modeling solar diffuser data for an instrument using solar calibration. It should be noted that historically, solar irradiance data sets have differed significantly, depending on the wavelength. It is important to use a single solar irradiance reference data set to maintain consistency (Coddington et al., 2019; Lean et al., 2020). The current recommended data set is the Total Solar Irradiance Sensor (TSIS)-1 Hybrid Solar Reference Spectrum (HSRS) (Coddington et al., 2021), and was accepted by the Global Space-based Inter-Calibration System (GSICS) as an international standard (Stone et al., 2021). TSIS has been very recently updated to version 2 with minor adjustment to version 1 data in the form of a scaling factor, by updating solar line positions at wavelengths longer than 0.74 μm , and by extending wavelength coverage to span 0.115 to 200 μm (Coddington et al., 2023), with data available at https://lasp.colorado.edu/lisird/data/tsis1_hsr.

Most datasets are listed in Table 3 that support reflectance and help facilitate atmospheric correction. Bidirectional Reflectance Distribution Function (BRDF) models for vicarious calibration sites are used to make necessary normalization to address illumination and viewing geometry. It is further recommended that BRDF models used for surface reflectance be standardized to better support harmonization of surface products (Helder et al., 2018). Spectral libraries are important to spectroscopy algorithms, which can include apparent optical properties (AOP), such as spectral reflectance or albedo, or inherent optical properties (IOP), such as leaf or phytoplankton pigment-specific spectral absorption and suspended particle backscatter coefficients as a function of instrument spectral response. For contributed spectral libraries in which source spectrometers may vary and measurement protocols may differ, proper documentation of procedures and spectrometer performance should accompany shared reference data as metadata. An example of establishing shared protocols is the global community library for soils, an effort of the IEEE p4005 working group for soil spectroscopy (<https://sagroups.ieee.org/4005/>).

In addition to shared reference data or models, some ancillary or auxiliary data are necessary for algorithms, especially those employing radiative transfer models (e.g., atmospheric correction or water column modeling for benthic reflectance). These ancillary or auxiliary datasets may originate from other satellite data products or models. They can include gridded data that are frequently updated, such as meteorological data or remain relatively static, such as a digital elevation model (DEM) or bathymetry.

3 Pre-launch Characterization and Calibration

Some aspects of instrument characterization or calibration cannot be done well on orbit and thus an instrument must be thoroughly tested under controlled laboratory conditions before launch. Pre-launch instrument characterization and calibration data also demonstrate that an instrument is meeting performance specifications, providing time to consider solutions not possible after launch. Pre-launch characterization data are also critical to generation of geolocated, at-sensor radiometry and science products (e.g., Guanter et al., 2015; Polz et al., 2021). For instance, both the instrument's radiometric response and spectral response function may be needed to convert instrument counts to radiance because in-flight calibration using the Moon or Sun involves

irradiance predictions derived using the characterized instrument spectral response. Example pre-launch calibration and characterization tests are shown in Table 4.

Pre-launch characterization data are used in the development and generation of other science data products and hence constitute an important set of reference data sets to share for data product harmonization, as mentioned in Section 2.3. Polarization and spectral responses can be used to create look-up tables used in common atmospheric algorithms, especially for observation of aquatic targets. Spectral response is used to predict the solar irradiance present for each band to compute surface reflectance and as input to some atmospheric algorithms. These data are also used by algorithm developers to transform spectral libraries to match the sensor bandpasses. However, two spectral responses may need to be made available to algorithm developers for the spectrometer: one based on the actual response of the spectrometer and one idealized spectral response for the corrected instrument using the Zong et al. (2006) stray light correction, the latter being most likely what will be employed by most algorithms.

Ultimately, calibration and pre-launch instrument characterization should be done to achieve accuracy needed (e.g., Polz et al., 2021), ideally dependent on the science questions or data applications that will be addressed (Thompson et al., 2021). Some tests will be conducted at component level (also called *piece-parts tests*), while others are done at the instrument system level or spacecraft integrated level. Most tests are performed in ambient, laboratory conditions, but radiometric testing sensitive to temperature is done in a thermal/vacuum chamber (Datla et al., 2011; Tansock et al., 2015). Ideally, they will follow the “test as you fly” approach (Datla et al., 2011), which posits that instruments should be calibrated as closely as possible to the same environmental conditions expected during operation. Standard ground support equipment and calibration sources will be used to ensure traceability and repeatability.

Table 4. *Common Pre-launch Calibration and Characterization Tests*

Radiometric Performance
Count-to-radiance gain (T/Vac)
Radiometric range (L_{min} , L_{max})
Saturation radiance (L_{sat})
Dark current characteristics
Linearity
Stability
Repeatability
Reproducibility
Noise characteristics
Signal-to-Noise Ratio (SNR) function
Polarization response
Spectral Performance
Spectral Response Functions (SRF) - In-band
Spectral Response Functions (SRF) - Out-of-Band (OOB)
Crosstalk
Spatial Performance
Instrument alignment and pointing
Near-field response
Far-field response
Band to Band Registration (BBR)
Modulation Transfer Function (MTF)

Pre-launch calibration and characterization tests can be expensive and time consuming because they require lengthy collections of data and rigorous analyses, thus they must be planned judiciously and well in advance of launch. The count-to-radiance gains are done in a thermal/vacuum chamber (T/Vac) at two or more temperature plateaus targeting the nominal operating temperature and bracketing the expected operational temperature range of the instrument. More detailed study of the instrument radiometric performance is done in an ambient temperature and pressure environment to better understand instrument feature linearity, stability and noise characteristics. In addition to the tests in Table 4, additional design-specific tests may be added to address possible instrument artifacts. Artifacts can include characterization of change in response as a function of scan angle, detector uniformity, or specifically for spectrometers, spatial ‘keystone’ or spectral ‘smile’ responses (Mouroulis & McKerns, 2000). Structured stray light artifacts such as ghosting need to be quantified and modeled (e.g., Zandbergen et al, 2020).

Ambient tests also included spectral, polarimetric and spatial responses. Spectral response characterization looks at the in-band (≥ 0.1 % response) and out-of-band (< 0.1 % response) at the same or lower spectral resolution than the in-band characterization. A monochromator or tunable laser can be used to measure spectral response of a spectrometer for all bands simultaneously. If the spectral response is easy to model from the instrument design, the experimental design is more straightforward. Communication between bands, or crosstalk, can also be quantified during such testing. The resulting set of spectral response functions would ideally be used to model the spectral response for all bands, which for the spectrometer is needed for the recommended stray light correction described by Zong et al. (2006).

Radiometric sources used are typically SI-traceable FEL lamps with a 10 or more cm aperture integrating sphere. It is possible to combine radiometric and spectral responses during characterization using a tunable laser reference (Ahtee et al., 2007), such as spectral irradiance and radiance responsivity calibrations using uniform sources (SIRCUS) (Brown et al., 2006) or Traveling SIRCUS (T-SIRCUS) or the Goddard Laser for Absolute Measurement of Radiance (GLAMR) systems (Angal et al., 2016; Barsi et al., 2019). This combined radiometric and spectral response is called the absolute spectral response (ASR) (Barnes et al., 2015). Measuring the instrument ARS potentially could reduce costs by combining testing steps and should be explored when designing a test plan for SBG pre-launch testing. Further, these calibration resources are transportable and can be shared with collaborating space agency missions.

Instruments such as spectrometers tend to change radiometric response with the polarization state of incoming light. The polarization response test, which pertains to VSWIR wavelengths only, is best kept simple, such as situating a sheet polarizer (with well-known spectral and polarimetric transmission) between the radiometric source and the instrument and rotating the polarizer to a set of angles (Waluschka et al., 2015). Typically, TOA light is polarized up to 70% across most visible and NIR wavelengths because of molecular scattering in the atmosphere (Meister et al., 2005). Variation in polarization yields a systematic radiometric artifact, which some observations are sensitive to, including dark aquatic targets. Correction of TOA measurements

that are critical to the quality of aquatic observations are usually done in the atmospheric correction over water using these characterization data (Meister et al., 2005).

Spatial response tests often use slit or cross reticles in front of a collimated beam providing near-field response (NFR), modulation transfer function (MTF), and band-to-band registration (BBR). Far-field response is more difficult because it requires placing bright sources in the periphery or outside of the instrument's field-of-regard and sufficient signal is difficult to achieve. Priority for implementing this test is design dependent. Additional testing of alignment, pointing, NFR and MTF provide mostly geometric and spatial characterization of the instrument. BBR, however, yields information on the radiometric and spectral quality of data from the sensor because the radiometric-spectral information from a spatially varying scene can become mixed if the bands are measured from different parts of that scene. MTF or BBR can be monitored and accounted for, but cannot be improved in orbit. Therefore, pre-launch testing is crucial to understanding these characteristics.

4 Orbit Planning - A Calibration and Validation Perspective

4.1 Calibration Opportunities with Other Missions

The SBG CVWG, in its efforts to develop a calibration concept, has placed considerable emphasis on the need to cooperate with other US and international VSWIR and TIR Earth imaging missions. One of the challenges that lies ahead for SBG and its cooperating missions, is the ability to optimize ground tracks from satellites in near-polar-orbits to image the same terrain and aquatic regions simultaneously or near-simultaneously and minimize differences in time of observation. Such approaches facilitate opportunities to achieve consistent measurements between instruments and build radiometric measurement performance confidence for the science and application communities who depend upon both high spectral resolution and high temporal revisit frequency. This approach of using sensor inter-comparisons is best achieved by selecting Earth regions where simultaneous nadir observations (SNOs) or near-simultaneous nadir observations (NSOs) occur, reducing atmospheric and solar illumination angle differences, that also can align with well-established radiometric and spectral calibration reference sites (Cao & Heidinger, 2002; Cao et al., 2004, 2005). SNOs can be computed using online tools, such as NOAA's tool found here <https://ncc.nesdis.noaa.gov/VIIRS/SNOPredictions/index.php>.

Differences in time and geometry between the sensors directly affects the uncertainty of any inter-consistency, inter-calibration or inter-validation derived from matching observations between two or more instruments. In practice, orbital characteristics place tight constraints on time and geometric differences, but this can drastically reduce the number of such observation matches, especially when orbits are less conducive to coincidental observation (see analysis below regarding PACE). In most cases, where the differences in time or geometry cannot be adequately constrained for calibration accuracy objectives, NSOs can still be used to inter-validate science data products created from the two or more sensors. In addition, the effectiveness of SNOs or NSOs to provide inter-calibration between two or more sensors or inter-validation between their data products depends also in part on the occurrence frequency of SNOs or NSOs, which in turn depends on the orbital characteristics of the sensors and to an extent the satellite swath width when geometry is left less constrained.

Ideally, observations for inter-calibration will be frequent, globally distributed, and cover surfaces suitable for inter-calibration. The SBG CVWG designed and conducted a series of NSO orbital simulations for both SBG VSWIR and TIR measurement concepts to characterize the challenges, opportunities, and limitations that can be anticipated during mission development and implementation. Our objective was to leverage knowledge of existing and notational mission orbits, whether descending or ascending, and their defined parameters to simulate the possibilities for Sun-synchronous Earth imaging in an effort to constrain the proposed SBG inter-calibration approach. We used the Systems ToolKit™ (<https://www.ansys.com/products/missions/ansys-stk>) to simulate daytime land imaging using orbital altitude, revisit frequency, and swath widths for SBG VSWIR and TIR imaging during the northern spring equinox period. The land area was covered with a 0.2° grid and coverage was computed if any portion of the swath touched the grid boundaries. We studied five specific SBG NSO scenarios with examples of potential cooperating missions. Comparisons in this study look primarily at terrestrial observations, however, matching aquatic observations would be comparable in frequency and use, albeit primarily for aquatic or other applications based on dark targets. The orbital parameters for missions under development, including SBG, are notional as of the time of writing this paper and may be subject to change. **Earth observation mission details and orbital parameters can be centrally accessed at Ramaseri Chandra, et al., 2022 and online at <https://calval.cr.usgs.gov/apps/compendium>.**

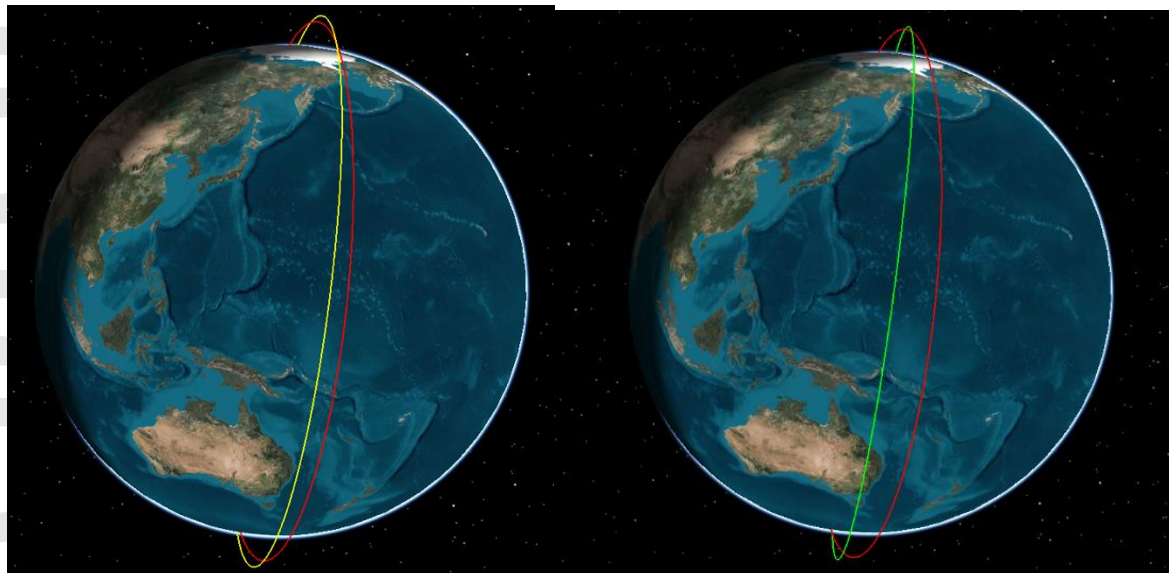


Figure 1. The left image depicts Sentinel-2a (yellow) 10:30am and Surface Biology and Geology (SBG) Visible-to-Shortwave Infrared (VSWIR) (red) 10:45am equatorial crossing times. The right image displays Landsat 8 (green) 10:12am and SBG VSWIR (red) 10:45am equatorial crossing times.

4.1.1 Scenario One: Crossing Time Difference between SBG VSWIR, Landsat 8, and Sentinel-2a

The SBG VSWIR reference orbit was placed at 619 km with a nadir repeating Sun-synchronous orbit (SSO) ground track at 16 days. The equatorial crossing time at the descending node was chosen to be 10:45 am local time with an instrument swath width of 185 km to ensure global observational coverage. Landsat 8 operates in a repeating SSO at an altitude of 705 km with a nadir repeat of 16 days and equatorial crossing time of 10:12 am local time (Roy et al., 2014). The Landsat 8 Operational Land Imager (OLI) has a 185 km swath width (Irons et al., 2012). The Landsat 8 OLI and SBG VSWIR instruments have an equatorial crossing time difference of more than 30 minutes as shown in Figure 1. These observations were simulated for a period of 48 days to compute NSOs occurring within 20 minutes (See Figure 2). Other inter-calibration studies using NSOs have allowed longer durations between image pairs, e.g., 30 minutes in Gil et al. (2020). However, 20 minutes was chosen as roughly one half of the daylight portion of an SBG orbit: time period of one SBG orbit is 97.06 minutes. The Landsat 8 OLI and SBG VSWIR NSOs occur only at high latitudes due to the differences in the equatorial crossing times. Sentinel-2a operates at an altitude of 786 km in a SSO with a nadir repeat of 10 days and an equatorial crossing at 10:30 am local time (Drusch et al., 2012). Sentinel-2a's Multi-Spectral Instrument (MSI) has a swath width of 290 km (Drusch et al., 2012). The SBG VSWIR and Sentinel-2a MSI observations were simulated just as done for Landsat 8 OLI. The NSOs in this comparison occur over the entire range of latitudes across the globe and are evenly spaced (See Figure 3).

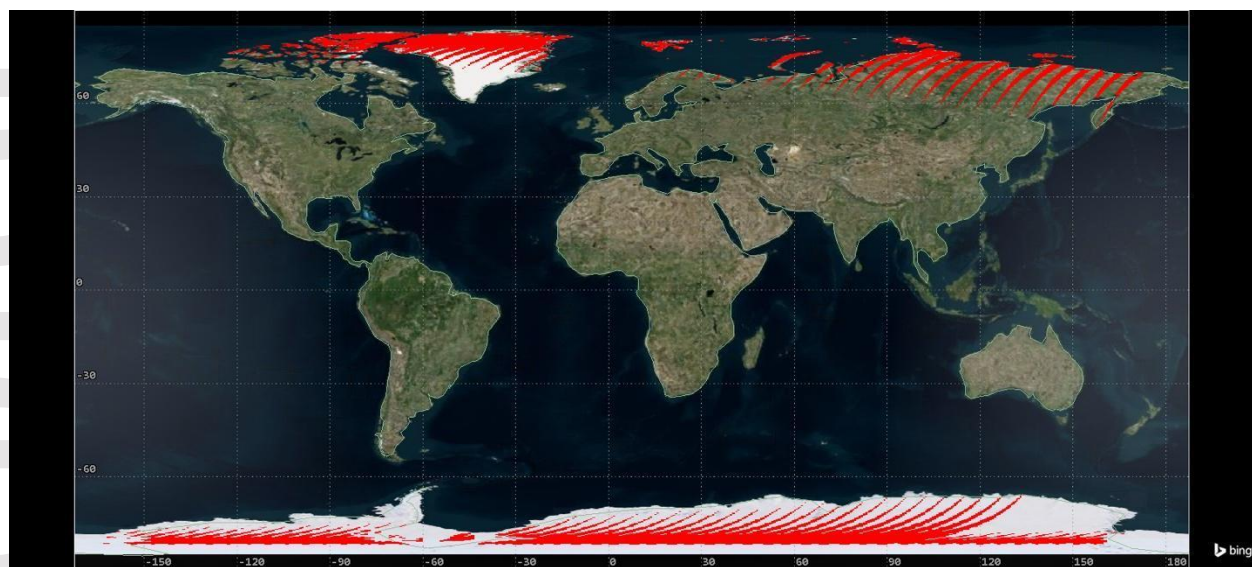


Figure 2. Near-Simultaneous nadir Observations (NSO) of Landsat 8 Operational Land Imager (OLI) and SBG VSWIR during a 48-day period centered on the northern spring equinox.

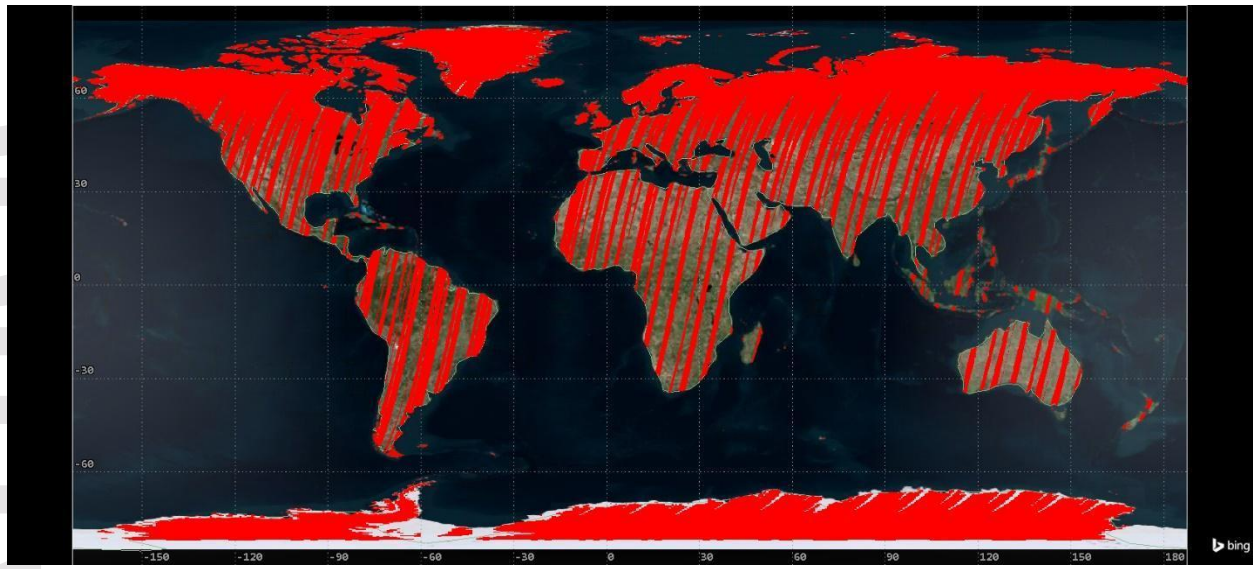


Figure 3. NSO of Sentinel-2a MultiSpectral Imaging (MSI) and SBG VSWIR during a 48-day period centered on the northern spring equinox.

4.1.2 Scenario Two: Descending SBG VSWIR and Descending CHIME

The SBG VSWIR reference orbital parameters above were used to compare NSOs occurrence with the CHIME mission. The CHIME orbital altitude was specified at 632 km with an equatorial crossing of 10:45 am local time ([ESA CHIME Mission Requirements Document v3.0, 2021](https://esamultimedia.esa.int/docs/EarthObservation/Copernicus_CHIME_MRD_v3.0_Issued_21_01_2021.pdf), https://esamultimedia.esa.int/docs/EarthObservation/Copernicus_CHIME_MRD_v3.0_Issued_21_01_2021.pdf, <https://space.oscar.wmo.int/satellites/view/chime>). The swath width was defined at 125 km with a 22-day SSO nadir repeating ground track. The SBG VSWIR and CHIME NSO opportunities are shown in Figure 4 and indicate where both instruments are imaging land regions within 20 minutes of each other. This comparison shows a tendency for higher NSO coverage over higher latitudes and polar regions, but evenly spaced NSO also occur across mid-latitude and equatorial regions during the 48-day period. Because SBG VSWIR and CHIME observatories are flying close in altitude, there are systematic 8 to 10 day intervals in NSOs (Figure 5) which are offset across the land surface.

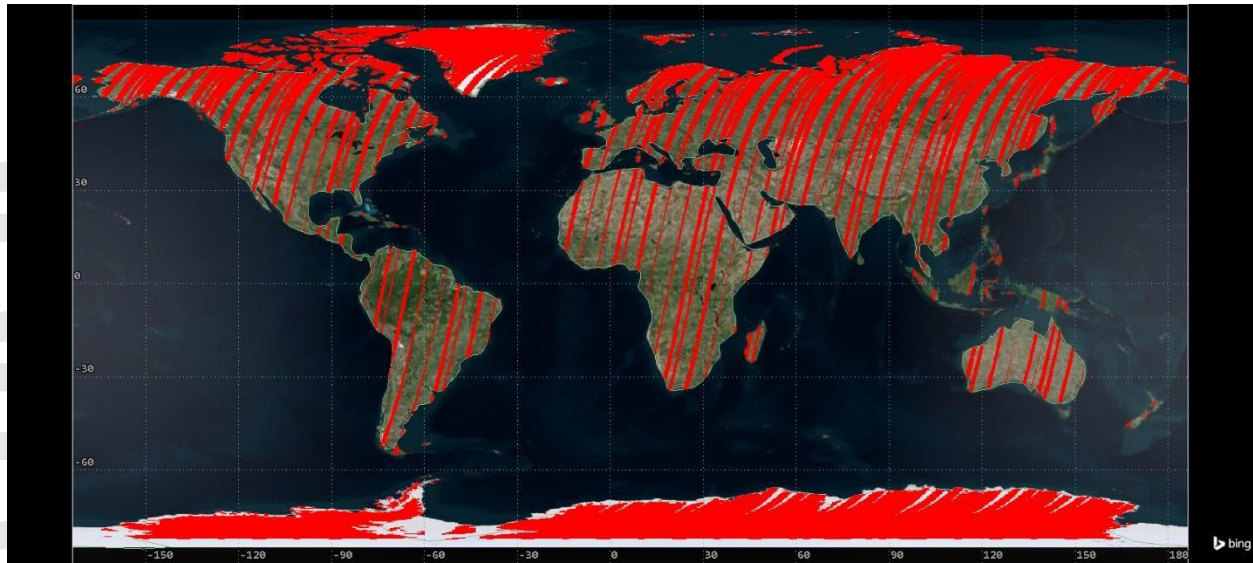


Figure 4. SBG VSWIR and CHIME NSO during a 48-day period centered on the northern spring equinox.

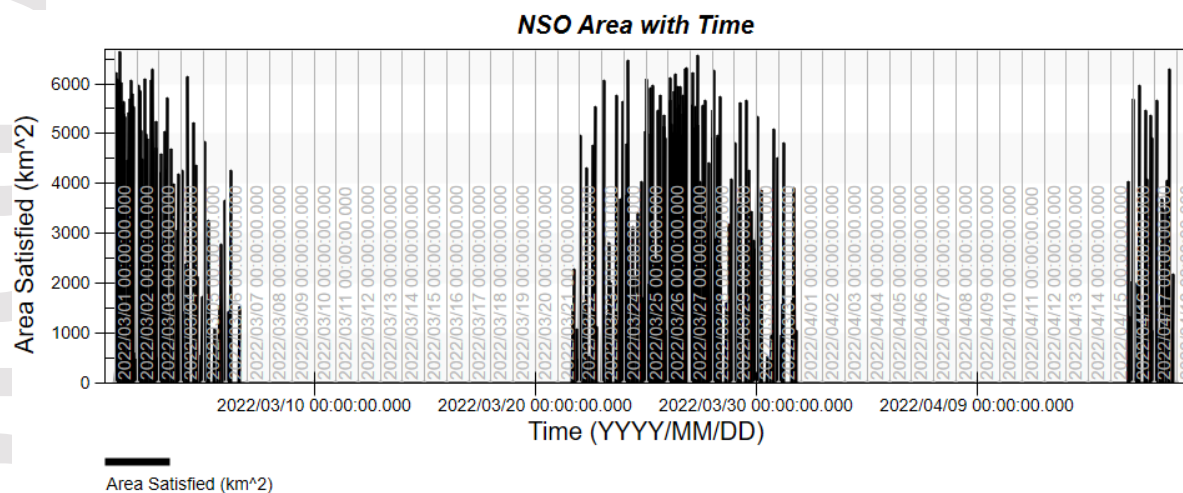


Figure 5. Periodic NSO land imaging occurrences between SBG VSWIR and CHIME missions during the 48-day northern spring equinox period.

4.1.3 Scenario Three: Descending SBG VSWIR and Ascending PACE

The SBG VSWIR reference orbit was compared with the ascending node of the PACE Ocean Color Instrument (OCI) to obtain NSO's opportunities. The PACE mission is in a SSO at an altitude of 676 km with an equatorial crossing of 1:00 pm local time (Werdell et al., 2019). The swath width of PACE OCI is 2,663 km at nadir which enables global imaging coverage at less than two days. The NSOs for SBG VSWIR and PACE OCI occur only at northern latitudes where their swath width would intersect during the daytime and Figure 6 shows the intersection of their orbital ground tracks. Figure 7 highlights NSOs between SBG VSWIR and PACE OCI at northern latitudes. It should be noted that the fact that NSO matches occur at all largely is because of the width swath of PACE OCI. But this also means that the geometries for matched

observations are likely very different. Thus, PACE cannot be used as a radiometric transfer instrument for SBG. However, relatively dynamic science data products (e.g., water-leaving reflectance) could be compared in the northern hemisphere.

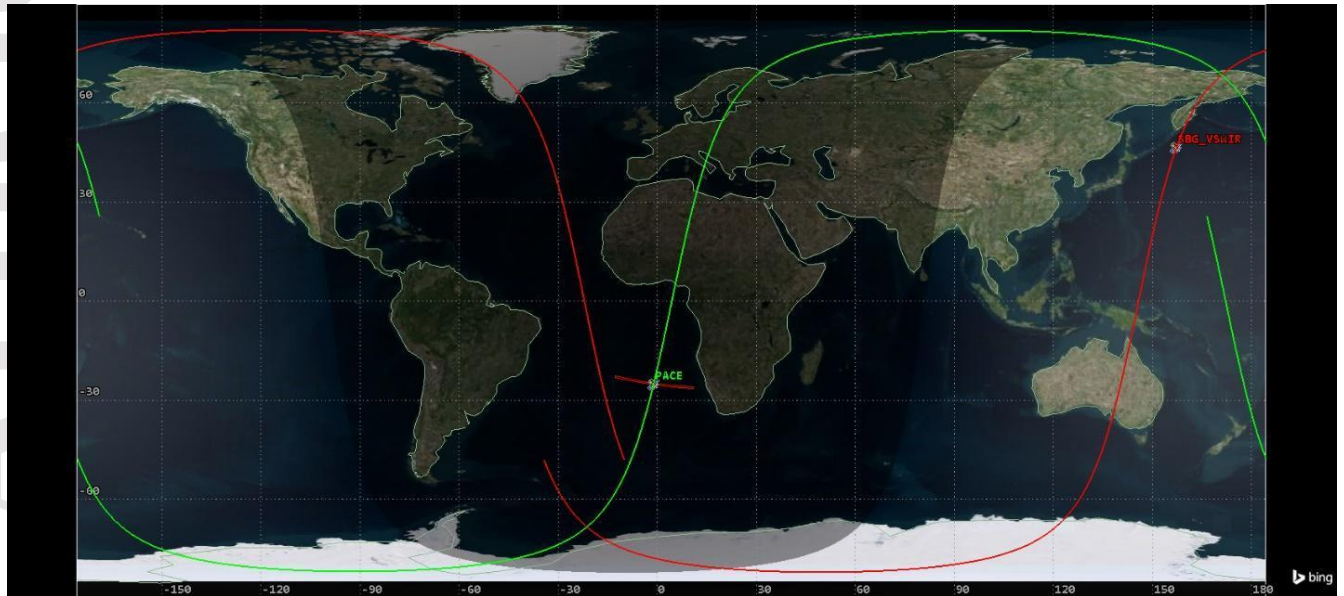


Figure 6. Ascending and descending orbit configurations for Phytoplankton Aerosols Clouds and ocean Ecology (PACE) (green) and SBG VSWIR (red).

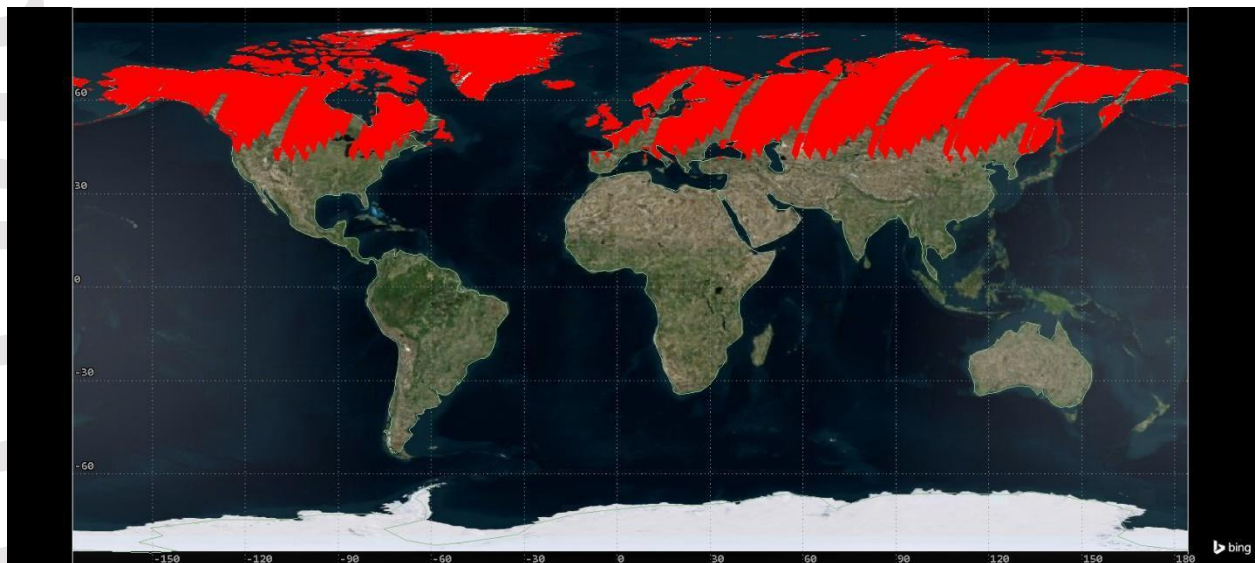


Figure 7. NSO PACE OCI and SBG VSWIR during a 48-day period centered on the northern spring equinox.

4.1.4. Scenario Four: Ascending SBG TIR and Descending Land Surface Temperature Mission (LSTM) TIR

The SBG TIR reference orbit was placed into a 666 km repeating ascending SSO with a nadir repeat of three days and an equatorial crossing of 1:30 pm local time. SBG TIR swath width was defined to be 935 km. The LSTM TIR orbit is at 640 km with a four-day nadir repeat descending across the equator at 1:00 pm local time with a 684 km swath width (ESA LSTM Mission Requirements Document v3.0, 2021, https://esamultimedia.esa.int/docs/EarthObservation/Copernicus_LSTM_MRD_v3.0_Issued_20210514.pdf; <https://space.oscar.wmo.int/satellites/view/lstm>). The SBG TIR and LSTM TIR comparison was simulated for a 12-day period. The large swaths of these TIR instruments result in an increased number of NSOs across northern middle and equatorial latitudes because the equatorial crossing time difference is only 30 minutes (See Figure 8).

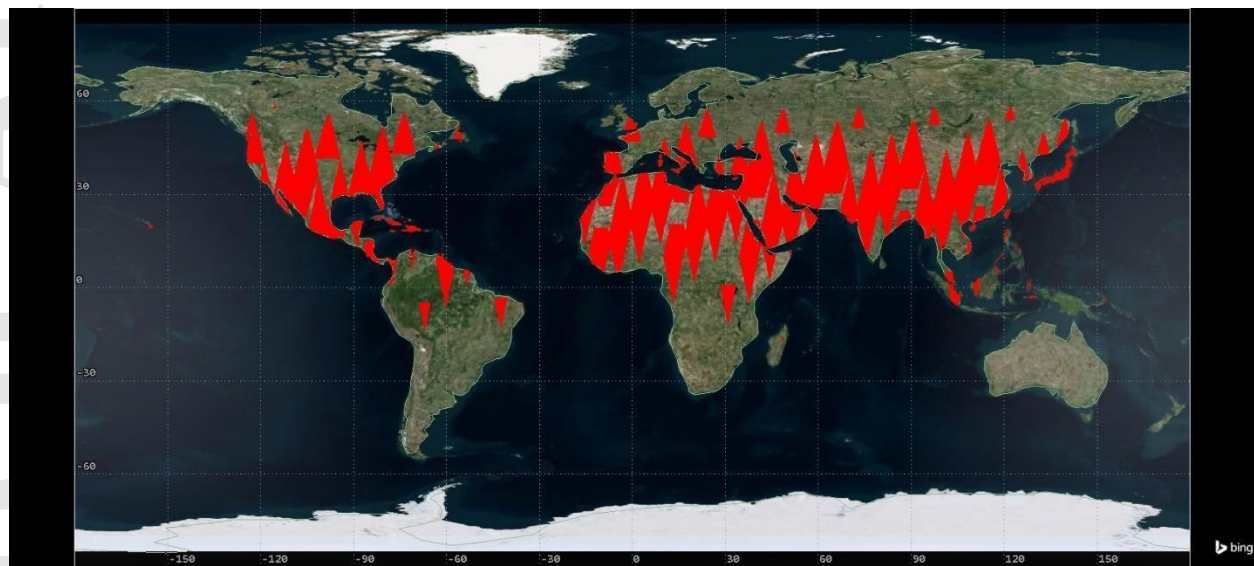


Figure 8. NSO of Land Surface Temperature Mission (LSTM) thermal infrared (TIR) and SBG TIR during a 12-day period centered on the northern spring equinox.

4.1.5 Scenario Five: Descending SBG VSWIR and International Space Station (ISS) CLARREO-Pathfinder (CPF)

The SBG VSWIR reference orbit remained the same as Scenario One, Two, and Three. CLARREO-Pathfinder will operate on the ISS at an altitude of approximately 400 km with an inclination of 52° with a swath width of 70 km (Shea et al., 2020; <https://clarreo-pathfinder.larc.nasa.gov/mission-overview/>; <https://www.eoportal.org/satellite-missions/iss-clarreo#mission-capabilities>) while SBG VSWIR is at an inclination of approximately 98° . The orbital planes of these two missions are nearly perpendicular and result in very small areas for NSOs. The number of NSO intervals are also much less compared to two opportunities that occur in a SSO. The latitudinal coverage is also limited due to the north and south 52° imaging constraint due to the ISS orbit inclination. Figures 9 and 10 show the comparison of orbit configurations and the occurrence of NSOs between CLARREO-Pathfinder and SBG VSWIR instruments over a 48-day period.

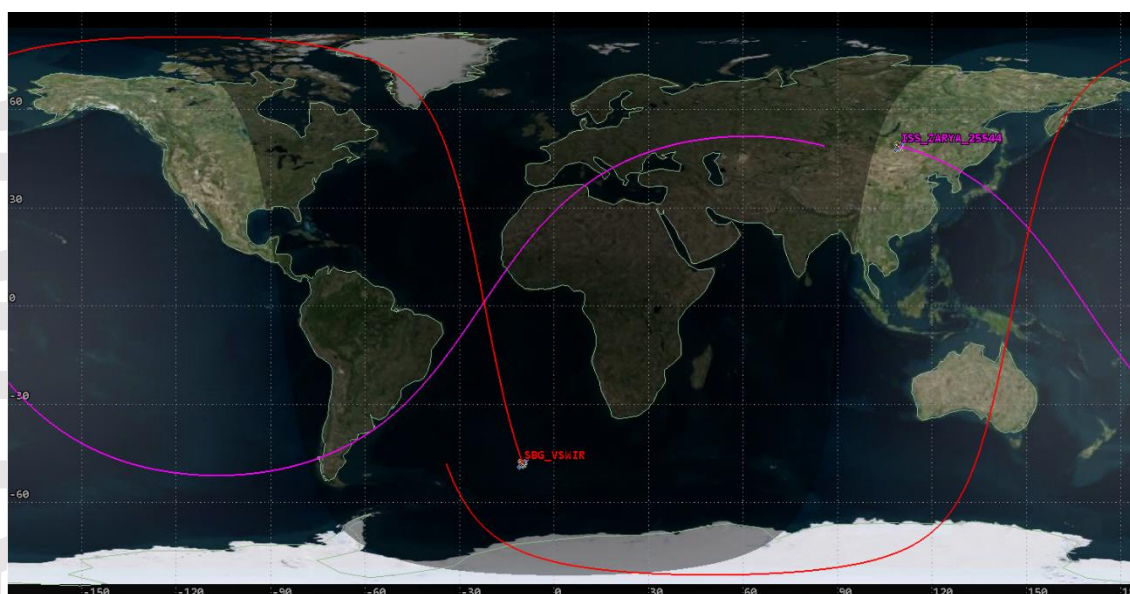


Figure 9. Descending International Space Station (ISS) orbit configurations for Climate Absolute Radiance and Refractivity Observatory (CLARREO)-Pathfinder (pink) and SBG VSWIR (red).



Figure 10. NSO of Climate Absolute Radiance and Refractivity Observatory (CLARREO)-Pathfinder and SBG VSWIR during a 48-day period centered on the northern spring equinox.

The SBG CVWG orbital simulations for SBG VSWIR and TIR instruments reveal some key findings regarding inter-calibration among cooperating missions for enabling science quality data. First, orbital altitude, imaging revisit frequencies, and imaging swath width of existing and planned space architectures for Earth imaging clearly point out the need for more synergistic

cooperation around designed SNO or NSO opportunities to maximize cross-mission capabilities if inter-calibration is a strategic mission priority for enabling science capabilities. Second, there are clear geographic imaging patterns that emerge across the global domain based on the current portfolio of existing and planned US and international VSWIR and TIR measurements, and while these occurrences may result in ad-hoc science and application utility, the current identified NSO maybe not align very well with the established ground-based radiometric calibration reference sites that are currently used in terrestrial remote sensing calibration and validation. Finally, SSO equatorial crossing times that exceed 20-minute NSO intervals, coupled with orbital ground tracks of the same revisit frequencies provide very limited inter-calibration opportunities except for polar regions. The SBG CVWG recommends better mission cooperation between US and international space agencies to optimize orbits in support of inter-calibration and higher quality terrestrial remote sensing science and application data products. This would require a balance between facilitating some simultaneous observations, while maintaining a sufficient offset to improve temporal sampling of the combined observations. This could be accomplished by choosing orbits with different revisit times that provide occasional alignment. However, in all cases, there are likely a significant number of opportunities for science data product inter-comparison or inter-validation.

4.2 Orbit Planning for Geometric Characteristics

The VSWIR imaging spectrometer and a TIR imager are planned to fly in a late morning and an early afternoon, Sun-synchronous, retrograde, integer-day ground track repeating near-polar orbit. On-orbit operations through regular drag make-up and inclination adjust maneuvers will maintain orbit altitude, eccentricity, inclination, local time at ascending or descending node, ground track repeatability accuracies to within tight margins (Bilimoria & Krieger, 2011). The instrument designs will take the Earth rotation, inclination angle, and variations of altitude and satellite speed along the sub-satellite point track into account so that ground coverage from the instruments will not have underlaps in either the cross- or along-track direction (Lin et al., 2016, 2018, 2019).

5 Calibration and Monitoring

5.1 Commissioning and Long-Term Monitoring

After the satellite is launched into an initial orbit altitude, there will be a series of orbit raising and inclination adjustment maneuvers to attain the nominal planned orbit altitude and inclination. In the meantime, an early orbit check-out (EOC) campaign will be conducted. That includes activation of GPS receivers, attitude determination and control sub-system, and possibly instruments, among others. This can include testing of onboard calibration systems, such as lamps or a blackbody source (after thermal detectors have been adequately cooled). After EOC, an intensive calibration and validation (ICV) campaign follows. The ICV establishes a baseline of calibration coefficients. During this phase, any onboard solar calibration system can be tested and further characterized in orbit using spacecraft maneuvers that move the Sun across these solar calibration system field-of-view. For example, primary EnMAP calibration has been done using onboard systems (Wilkens et al., 2017) while validation relies, in part, on the cooperation with experienced international partners, and data from established calibration, validation and monitoring sites and networks detailed in following sections, as well as on intercomparison of

data from other missions (Brell, et al., 2021). Long-term monitoring corrects for drifts of calibration coefficients. Periodic ICVs may establish updates to calibration, for example, Masek et al. (2020) describe a combination of sensor intercomparisons, use of the AEROSOL ROBOTIC NETWORK (AERONET), Surface Radiation Budget Network (SURFRAD), and buoy networks, and comparison with field spectroscopy and airborne imaging spectrometer data to validate Landsat Level-2 surface reflectance and surface temperature products.

To harmonize data sets from multiple missions, inter-calibration on-orbit using common references is critical. The Moon can potentially facilitate inter-calibration over long periods of time, provided current efforts successfully improve models of lunar irradiance to become SI traceable and <1% accuracy or better (Stone et al., 2021). It is potentially an ideal target because its measurement is not influenced by the Earth atmosphere or anything that can be significantly influenced by changes in the Earth's climate (this is discussed further in the next section). Observations of the Earth with near identical timing and geometry could also support true inter-calibration in the short term provided the surface target is well known at the top of the atmosphere (e.g., the target has a very predictable BRDF and the atmospheric optical column above the target is accurately measured and modeled). However, atmospheric effects could be influenced by long-term climate changes and thus limit the Earth as an ideal target for long-term inter-calibration for high levels of accuracy.

Achieving radiometric scale agreement between instruments not only depends on the quality of the radiometric knowledge of the reference observation, but accuracy of the spectral and geometric calibration. Errors in wavelength positions of spectral channels can translate into radiometric errors (depending on the slope of the reference spectrum with respect to wavelength). Misaligned imagery can likewise lead to radiometric errors (depending on the radiometric partial derivatives of the image with respect to raster dimensions). Therefore, it is important to first address the spectral and geometric calibration using common references before inter-calibration and data harmonization, which require common spatial and spectral grids.

Spectral calibration can be monitored on-orbit using onboard reference sources (Micijevic et al., 2022) or external reference targets. External references could include gas absorption lines caused by the Earth's atmosphere (Green et al., 2003; Kuhlmann et al., 2016; Richter & Schlapfer, 2019). In addition, minerals with strong, narrow absorption features at the Earth's surface could also serve as spectral calibration targets. Examples of such targets include the long-utilized geologic remote sensing reference site at Cuprite, NV (Swayze et al., 2014) and the site at Makhtesh Ramon, Israel (Pearlshtien et al., 2021; Pearlshtien and Ben-Dor, 2022). Fraunhofer lines appear in lunar or solar observations, in cloud and ice reflectance, or in specular reflectance off water. But the spectral features of the solar spectrum are too fine-structured to adequately resolve given the SBG VSWIR expected ~10 nm spectral resolution over its 380 to 2500 nm range (see Figure 11). However, as demonstrated in Figure 11, the SBG VSWIR spectrometer could perhaps monitor atmospheric absorption features, which would be observed for bright targets on Earth.

Reference features in spectra, such as absorption lines, are well defined by well-known laws of physics, are very predictable and so instrumentation or modeling is less necessary for target sites on the Earth's surface. Geometric calibration of the instrument line-of-sight can also be refined in orbit during the commissioning phase using surface features such as narrow bridges,

established reference ground control targets, or even high-resolution reference imagery such as digital orthophoto quadrangles (DOQ). However, radiometric calibration is more challenging because most potential calibration targets found on the Earth's surface are subject to some degree of change (and changing reflectance or temperature are characteristics of the very phenomena that we seek to measure). Finding stable, well-known references for the radiometric scale can hence be especially challenging.

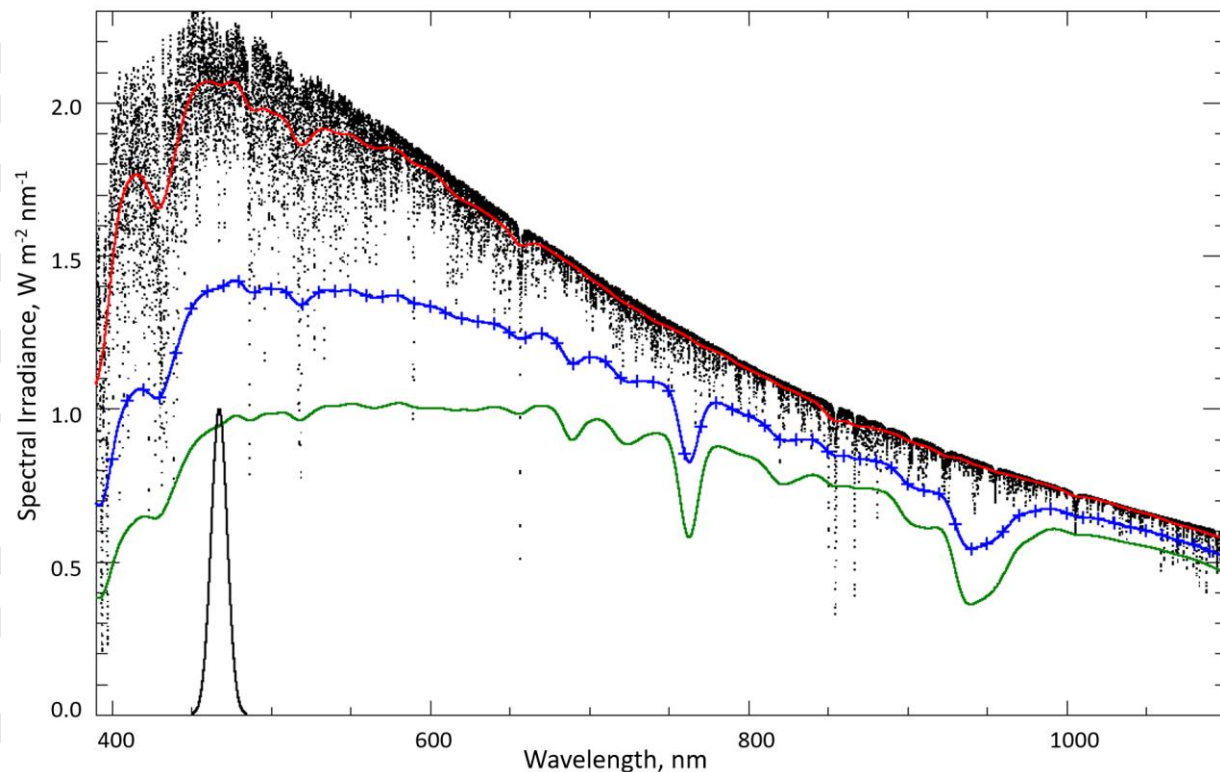


Figure 11. Simulated Surface Biology and Geology (SBG) spectra. The black dots are the Total Solar Irradiance Sensor (TSIS)-1 Hybrid Solar Reference Spectrum (HSRS) solar spectrum at 0.1 nm resolution (Coddington et al., 2021, 2023), showing most of the solar structure. Fraunhofer lines are about 0.4 nm wide, e.g., H α at 656 nm. The colored lines show simulated measurements by convolving with a Gaussian shape with a nominal full-width-half-max (FWHM) of 10 nm. The black line near 470 nm shows the 10-nm spectral response profile used. The red line is a simulated measurement of the exo-atmospheric solar irradiance spectrum. The blue line simulates the same measurement of exo-atmospheric solar irradiance after one pass through a typical atmosphere over-land atmosphere based on MODerate resolution atmospheric TRANsmission (MODTRAN) (Anderson et al., 2000); the plus signs indicate nominal bands at 10 nm spacing. The green line simulates the same measurement with two passes through the same modeled atmosphere.

Vicarious calibration involves special *in situ* data (not used for validation) to characterize the satellite sensor response. Much of the same or similar *in situ* instrument infrastructure is used for acquiring these data. As with validation, the calibration plan should also leverage existing best practices, resources, techniques, and protocols. Vicarious calibration also typically requires

modeling to provide TOA radiance or reflectance to compare against satellite observations. This means that a vicarious calibration plan must have input from the ground systems to be sure to use the same radiative transfer model that is being used operationally for atmospheric correction.

5.2 The Moon

Using the Moon as a full-system measure of responsivity changes for solar reflectance bands of on-orbit instruments has been a common and generally successful activity for the past quarter-century. Three major steps are involved: 1) acquiring an image of the Moon in all solar-reflective bands; 2) processing the image data to an apparent lunar irradiance; 3) comparing the measured irradiance to a spectral-irradiance model of the Moon. Each of these steps has challenges, often unrecognized, which has limited the effectiveness and the acceptance of lunar calibration. These challenges are rapidly being addressed and lunar calibration in the SBG era holds the promise of sub-percent absolute calibration and trend capability (Kieffer, 2022; Stone et al., 2020), including the current airborne LUnar Spectral Irradiance (air-LUSI) mission (Woodward et al., 2022).

The Moon can be considered a reference diffuser of accurately known size, with sharp edge on half its circumference, zero background and weak broad spectral features. Its reflectance is similar to soil. It is also essentially unaffected by Earth climatic change, whereas earthbound instrumented sites and the propagation of surface measurements to TOA potentially are. The stability of its overall reflectance, 10^{-8} /annum (Kieffer, 1997), is better by several orders of magnitude than artificial surfaces. However, lunar irradiance varies widely with geometry and a model is required; this relation is conceptually knowable to great accuracy and precision. Total lunar spectral irradiance for a given set of illumination and viewing angles and distances can be modeled empirically based on prior lunar irradiance characterization as a function of geometry. Such a lunar spectral-irradiance model (Kieffer and Stone, 2005) has been in common use for nearly two decades. For instance, the Sea-viewing Wide Field-of-view Sensor (SeaWiFS) mission used the Moon exclusively to perform a time-dependent calibration in orbit to within 0.2% uncertainty (Eplee et al., 2006). Improved lunar models are an active research area (Kieffer, 2021a, 2022; Stone et al., 2020; Sun and Xiong, 2021; Taylor et al., 2021; Wang et al., 2020). Lunar irradiance is polarized (Dollfus, 1962), up to several percent at common calibration geometries, passing through zero at phase angles near 24° . Although polarization could affect radiometric measurements, the polarization of lunar light has been largely ignored in lunar calibration because the expected effects would be very small. But modern measurements (see <http://calvalportal.ceos.org/lime-documents>) are being made after nearly a century gap.

Lunar calibration observations are best made by pointing the instrument directly at the Moon, using the same optical configuration as science observations. This commonly involves a spacecraft attitude maneuver and places requirements on spacecraft agility. A mission concept should plan on frequent lunar observations during the commissioning or start of a mission. Possible indirect effects of an attitude maneuver can be determined during commissioning; e.g., long scans crossing the Moon at several azimuths, scans in both directions, observations early and late along an orbit, and early and late in an attitude maneuver. It is important to be prepared for near-real-time analysis in case of unexpected artifacts, allowing them to be pursued during commissioning. Lunar observations should be conducted at least monthly in the first year. In subsequent years, the temporal repeat of lunar observations can be expanded if necessary.

However, if possible, lunar observations should be steadily collected and the frequency increased if any mission calibration or other event necessitates.

At present, lunar-calibration results differ substantially between many instruments (Kieffer, 2021b). The main suspect is differences in optical path between lunar calibration and normal science observations; these must be periodically calibrated by direct observations of the Moon. Because the Moon is static, a lunar observation at any time, even years ago, can be used for a radiometric calibration and benefit from improving lunar models. An entire constellation could calibrate on the Moon with no simultaneity requirements and also the Moon can be used to calibrate sensors consistently for long-term observations of the effects of climatic change, even across a series of multiple missions.

Lunar observations also aid geometric assessments. Lunar images are unparalleled for the identification of 'ghosts' and bright-limb scans can track any degradation of MTF. The virtual zero background allows sensitive determination of off-axis response and quantifying the size-of-source effect, which is very difficult in the laboratory. Lunar scans were made to correct out-of-field stray light, or ghost effects, for the Landsat 8 Thermal Infrared Sensor (Montanaro et al., 2014).

5.3 The Sun

The Sun can serve as a source for calibrating instruments in flight. Like the Moon, it can facilitate both an absolute calibration of the instrument after the transfer to orbit and monitor the instrument calibration, supporting time-dependent calibration. The Sun has the advantage of being relatively stable over the VSWIR range to about one part in a thousand (Lean et al., 2020; Coddington et al., 2019) and with the more accurate knowledge of the solar spectral irradiance provided by the TSIS-1 HSRS (Coddington et al., 2021, 2023), the solar output has become a more accurate reference. Unlike the Moon, the Sun does not go through large changes that must be carefully predicted and it can be viewed anytime.

However, the main challenge of using the Sun is that it is several orders of magnitude brighter than the targets that Earth observing satellites are designed to observe. This is typically addressed by adding an optical element to step down the solar output before being observed by the instrument. A common approach is to use a uniform, isotropic reflective plate, called a solar diffuser. Diffusers can be spectrally near white or doped to be gray, further stepping down the solar signal. Doping can also add spectral features that can be used to monitor the spectral calibration of spectrometers on orbit, provided they have sufficient spectral resolution. Solar diffusers can be constructed of polytetrafluoroethylene (PTFE), and come in different levels of purity. Other diffuse materials or coatings can also be used, such as ceramics, quartz volume diffuser (QVD) or barium sulfate.

However, there is a key drawback with such a calibration system: the reflectance of the solar diffuser may not be constant, but change with exposure to the harsh environment of space and strong solar irradiation. These changes differ with material and manufacture. In all cases, a strategy to monitor the changes to the solar diffuser is critical to avoid the introduction of spurious trends in the Earth observations. One method to quantify changes to the diffuser in space is to situate a monitoring instrument to compare the solar diffuser at a similar viewing

geometry to what the main instrument sees during calibration and ratio that to light from the Sun attenuated with a screen. These devices are called Solar Diffuser Stability Monitors (SDSM) and have been used for the MODerate resolution Imaging Spectroradiometer (MODIS) (Xiong et al., 2014) and the Visible Infrared Imaging Radiometer Suite (VIIRS) (Fulbright et al., 2015) instruments. However, these monitoring instruments must be well characterized and stable or they will leave residual spurious trends in the solar time-dependent calibration. Another approach to the SDSM is to use two or more solar diffusers, one for frequency observation and another to be shielded and removed for observation much less frequently. The less frequently observed diffuser provides a baseline against which the more frequently observed diffuser can be compared and its changes monitored and removed from a time-dependent calibration. This approach will be used by the upcoming OCI ocean color spectrometer in the PACE mission. Finally, it is possible that lunar observations could be used to remove residual, spurious trends in the solar calibration time series (Eplee et al., 2019; Choi et al., 2022).

Also, unlike the Moon, because the solar diffuser can provide a broad uniform and isotropic source across the entire instantaneous field of view (IFOV) of the instrument, detector arrays can be checked for striping, depending on the instrument design. However, because exposure to solar radiation over time may not be consistent across the diffuser (or if there are any flaws in manufacture), the solar diffuser may not degrade uniformly, thus changing into a nonuniform or anisotropic source. There is no current design to monitor or accurately detect such phenomena, which could undermine characterization of differences between detectors.

5.4 The Earth

The SBG CVWG recommends that the NASA SBG project and its collaborating agencies identify or develop joint surface measurement networks. This would start with the identification of existing resources for validation or vicarious calibration data and determining any potential gaps or limitations. The agencies could work to share development of any additional resources needed and could also identify any airborne and spaceborne resources for calibration and validation of imaging spectroscopy or thermal infrared imagery. For surface, airborne and spaceborne assets, the NASA SBG project and its collaborating agencies could leverage current and emerging methods by identifying existing or developing new standard validation and vicarious calibration strategies and protocols. In this section, we consider some key examples for calibration and validation measurement resources on the Earth's surface.

Masek et al. (2020) recommended that efforts to characterize and validate Landsat Level-2 data products expand to beyond bright surfaces with dry atmospheres to regions where atmospheric compensation is more challenging to implement, and to bright and dark land surface targets beyond just deserts and vegetation (e.g., water bodies, bare soil, snow and ice, and impervious surfaces). To that point, EnMAP is validating surface reflectance with *in situ* reference measurements from selected, diverse core sites that span agricultural, aquatic, exposed geologic, and snow-covered surfaces (Brell et al., 2021). Because potential variation in the Earth's atmosphere increases uncertainty, care must be taken when using such references for time-dependent calibration because of atmospheric variations, especially when they can be influenced by climate change. For this reason, onboard or celestial references are preferred for on-orbit, at-sensor calibration (Storch et al., 2014) to support mission objectives such as change detection, monitoring, and trending, while vicarious measurements are employed for validation of data

products or for one time adjustments after transfer to orbit (Masek et al., 2020). For terrestrial applications, vicarious calibration has been used to evaluate and if necessary, adjust surface reflectance values retrieved through a radiative transfer algorithm (Matersperger et al., 2013; Clark, R.N., et al., 2002). For aquatic remote sensing, system vicarious calibration (SVC) is primarily used to offset biases in order to optimize accuracy of surface radiometry, not at-sensor accuracy. In this way, biases in the atmospheric radiative transfer model are incorporated into the adjustments applied to the calculation of water-leaving reflectance from TOA measurements (Clark et al., 1997) and this step is considered critical to accurate retrieval of water-leaving reflectance from space.

5.4.1 Terrestrial References

To characterize radiometric response of optical remote sensing systems, a number of tools and techniques are utilized, including pseudo invariant calibration sites (PICS), RadCalNet, SURFRAD, AERONET, and instrumented thermal calibration sites.

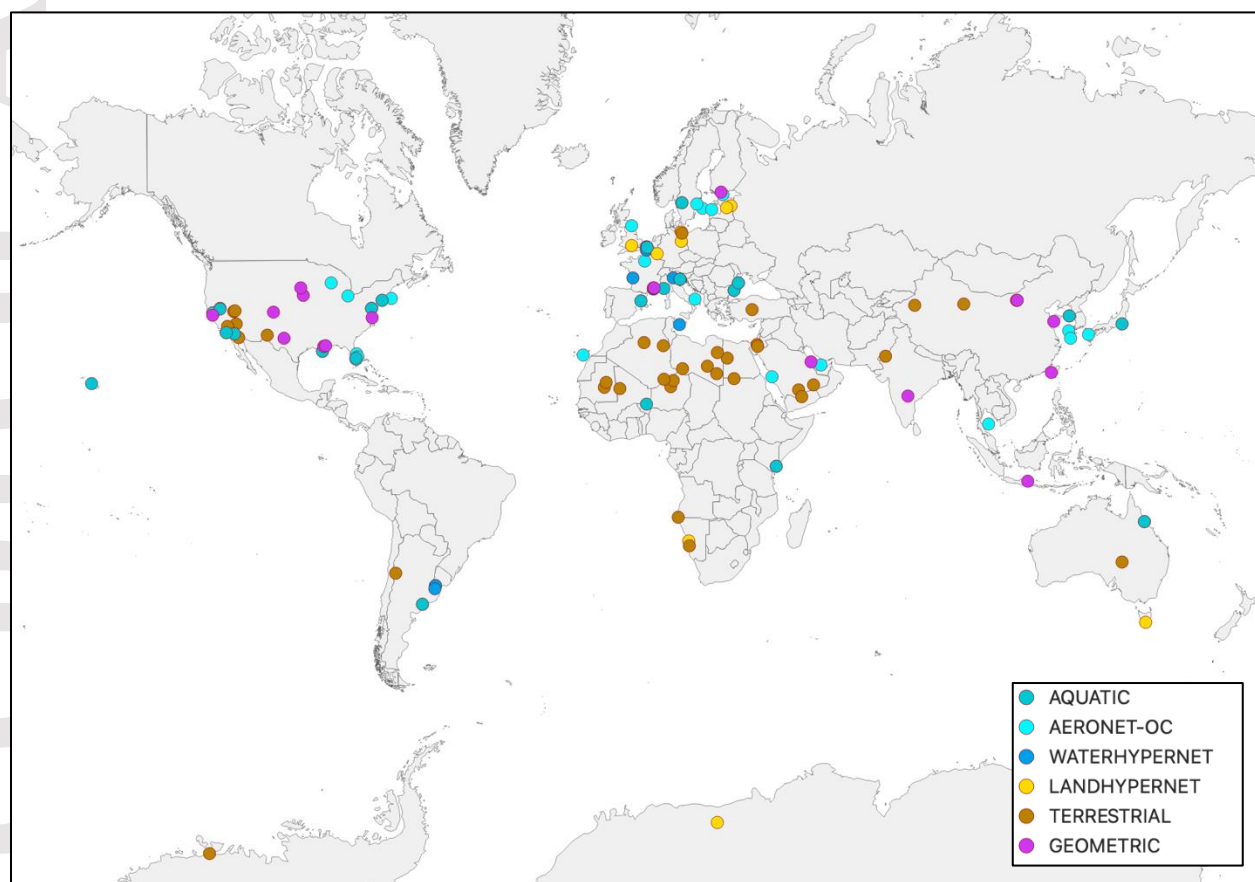


Figure 12. Calibration and Validation (CalVal) Sites – including global distribution of terrestrial radiometric and geometric sites maintained by US Geological Survey (USGS) used for Landsat, (<https://www.usgs.gov/tools/test-sites-catalog>), the LANDHYPERNET, and locations of aquatic remote sensing validation sites (AERONET-OC, WATERHYPERNET, and other Aquatic sites). Locations for most sites are provided in tables 5 through 7, except the HYPERNET sites provided by Ruddick (2023).

5.4.1.1 Radiometric Calibration Targets

Features of the Earth's surface such as inland ice sheets or targets well outlined by Chander et al. (2013), including pseudo-invariant surface targets, deep convective clouds, liquid water clouds, and sun glinted water bodies, have been used for various analytical purposes, including inter-comparisons and inter-calibration. Terrestrially, PICS are locations that are found to be highly radiometrically stable over time (Table 5). PICS of highest stability include flat sandy desert terrain, where geometric relief, atmospheric and surface moisture, as well as population and human-induced change, are all minimal. The general geographic distribution of candidate PICS can be seen in Figure 12. However, these locations can be impacted by adverse radiometric, spectral and thermal characterization conditions including metamorphosing surface, i.e., change in snow grain size and ice structure, poor illumination angle, solar geometry and increased atmospheric dynamics. At desert sites, spectral response and repeatability nominally measure within 1-3% depending on spectral band, viewing geometry and site (Cosnefroy et al., 1996; Helder et al., 2013). The CEOS WGCV has agreed upon and endorsed a set of six such desert PICS for long-term satellite monitoring and reference purposes, and more information can be found at https://calvalportal.ceos.org/pics_sites and within the PICS reports published therein. New PIC usage methodologies and techniques in evaluation stages include extended PICS (EPICS) and super or cluster PICS with the goal of increasing PIC scene analysis data (e.g., Khakurel et al., 2021; Vuppula, 2017).

The AERosol RObotic NETwork (AERONET) program (<https://aeronet.gsfc.nasa.gov>) was established by NASA and the Université de Lille Laboratoire d'Optique Atmosphérique in the early 1990s. AERONET is an atmospheric measurement network, but in some cases, it could potentially help characterize atmospheric effects in coincident calibration and validation surface sites. Surface-pointing instruments measuring reflectance can be situated at AERONET station (for example, see AERONET-OC in Section 5.4.2). The program characterizes and monitors aerosols, water vapor, and clouds at discrete calibration sites around the globe. The network provides openly available, long-term continuous data for use by several remote sensing missions, data products, airborne campaigns, and similar uses (Holben et al., 1998). The program continues to evaluate, curate data, and expand stations over time.

The RadCalNet (<https://www.radcalnet.org/>), an initiative of CEOS WGCV, is a network of radiometric calibration sites across the globe providing SI-traceable spectrally-resolved TOA reflectances including associated uncertainties to aid in-flight and on-orbit radiometric calibration and validation of Earth observation sensors operating in the (VSWIR) spectral region (Table 5). Currently, there are five such sites (two in China and one each in France, Namibia, and the USA) equipped with automated ground instruments making continuous measurements and are managed independently. The RadCalNet attempts to improve the temporal sampling issues that exist in on-orbit sensor calibration, provides global consistency, and increases the available calibration opportunities, by networking measurements from these sites. Bouvet et al. (2019) provides further information on data collection including their data processing approach and an example of inter-consistency study between two sensors using RadCalNet data. Alonso et al. (2019) describes the use of RadCalNet measurements in the validation of DESIS imaging spectrometer data. In addition, Czapla-Myers et al. (2020) discussed results of comparing several

space-borne sensors using the RadCalNet site located at Railroad Valley, Nevada, USA also known as Radiometric Calibration Test Site (RadCaTS).

The NOAA Global Monitoring Laboratory provides the SURFRAD Network of hourly Earth and atmosphere system radiation measurements across a wide network of stations in varying geographic and climate zones (<https://gml.noaa.gov/grad/surfrad/>). The program was established in the early 1990's with the aim of providing reliable field data to support remote sensing climate research. Primary measurement variables include upwelling and downwelling radiation, direct and diffuse solar, photosynthetically active radiation, UVB, spectral solar, and ancillary meteorological parameters (National Oceanic and Atmospheric Administration Earth System Research Laboratory, 1995).

The recently launched Landsat 9 and EnMAP missions utilized contributed data from collaborators across the globe for validation during commissioning phases. The utilization of contributed data from various sources places a secondary calibration/validation burden on the teams collecting field-measured data. Spectrometer characterization (spectral and radiometric) and measurement protocols should be established to ensure equitable data, for example, Malthus et al., 2019; Ong et al., 2018. However, the measurement protocol may vary between surface types, for example, water bodies versus bright soil or sediment surfaces. The recently deployed Field, Line-of-sight Automated Radiance Exposure (FLARE) network is a commercial system of satellite validation of geometric and radiometric performance (Durell & Russell, 2020).

5.4.1.2 Thermal Calibration Targets

Thermal emissive band calibrations are completed in addition to the solar reflective band calibrations. In contrast to the solar reflective region of the electromagnetic spectrum, thermal infrared energy observed by satellites is a measurement of Earth surface emitted radiance, as well as energy absorption and emission through the atmosphere (Czajkowski et al., 2000). Thermal emissive band calibration typically involves on-board blackbody observations and use of Earth surface aquatic and terrestrial calibration data (Hook et al., 2007; Xiong et al., 2009; Pérez Díaz, et al., 2021). Many current and forthcoming thermal Earth observation missions have used the long-term automated and complimentary thermal infrared calibration sites, for example at Lake Tahoe, CA/NV, USA and Salton Sea, CA, USA (e.g., Hook et al., 2020) (Table 5) and end-member high and low temperature or emissivity targets for calibration and validation purposes (e.g., Hall et al., 2008). Calibration and validation efforts typically use ground instrument measurements of thermal emitted surface radiance, atmospheric observations and a radiative transfer model to simulate the at-sensor equivalent thermal radiance values. These at-sensor simulated thermal radiances are then compared with actual on-board sensor measured radiance and assessed by thermal spectral band. Hulley et al., 2021, describe two primary methods for validation of land surface temperature and emissivity products, the classical Temperature-based approach (Wan et al., 2002) relying on instrumented sites and the Radiance-based method (Coll et al., 2009) applicable where emissivity is known, which were applied to ECOSystem Spaceborne Thermal Radiometer Experiment on Space Station (ECOSTRESS) data for fourteen land and water sites located in North America, Europe, and Africa. An international team of experts representing the CEOS WGCV have recommended two additional methods, multisensor intercomparison and time-series analysis approaches (Guillevic et al., 2018) which

are useful for comparing products generated from different algorithms and with different observational characteristics, and for observing long-term trends, biases, and atmospheric effects.

Table 5. *Global Terrestrial Sites Recommended for Vicarious Calibration*

Site Name	Location
Algeria 3	30.32°N, 7.66°E
Algeria 5	31.02°N, 2.23°E
Arabia 1	18.88°N, 46.76°E
Arabia 2	20.13°N, 50.96°E
Baotou Sand, BTSN*	40.8658°N, 109.6155°E
Baotou Sand, BTCN*	40.8517°N, 109.6289°E
Barreal Blanco*	31.86°S, 69.45°W
Demmin	53.90°N, 13.17°E
Dome C*	74.50°S, 123.00°W
Dunhuang*	40.13°N, 94.34°E
Egypt 1	27.12°N, 26.10°E
Ivanpah Playa*	35.5692°N, 115.3976°W
La Crau*	43.56°N, 4.86°E
Lake Tahoe*†	39.09685°N, 120.03235°W
Libya 1	24.42°N, 13.35°E
Libya 2	25.05°N, 20.48°E
Libya 3	23.15°N, 23.10°E
Libya 4	28.55°N, 23.39°E
Lunar Lake Playa*	38.40°N, 115.99°W
Makhtesh Ramon*	30.59°N, 34.84°E
Mali	19.12°N, 4.85°W
Mauritania 1	19.4°N, 9.3°W
Mauritania 2	20.85°N, 8.78°W
Namib Desert 1	24.98°S, 15.27°E
Namib Desert 2	17.33°S, 12.05°E
Negev*	30.11°N, 35.01°E
Niger 1	19.67°N, 9.81°E
Niger 2	21.37°N, 10.59°E
Niger 3	21.57°N, 7.96°E
Railroad Valley Playa*	38.5°N, 115.69°W
Rogers Dry Lake*	34.96°N, 117.86°W
Salton Sea*†	33.22532°N, 115.82425°W
Sonoran Desert	32.35°N, 114.65°W
Sudan 1	21.74°N, 28.22°E
Taklamakan Desert	39.83°N, 80.17°E
Thar Desert	27.63°N, 71.86°E
Tinga Tingana*	29.00°S, 139.86°E

Tuz Golu*	38.83°N, 33.33°E
White Sands*	32.92°N, 106.35°W
Yemen Desert	16.87°N, 47.55°E

*Currently Instrumented, †Thermal Site.

In thermal calibration and validation activities, water vapor is an important quantity that must be well characterized (e.g., for more details see Quattrochi and Luvall, 2004 and Xiong et al., 2020). Thermal emissive bands also must be well-calibrated for the ‘split window’ data algorithm technique which utilizes the difference in brightness temperature between targeted thermal emissive bands to correct for atmospheric effects as compared to measured Earth aquatic and land surface temperatures.

5.4.1.3 Geometric Calibration and Assessment

Instrument geolocation calibration starts when the first-light images become available, even before the nominal orbit altitude is attained. It is expected that the initial correction will be very large, in the order of thousands of microradians in the instrument-to-spacecraft mounting alignment angles that are thousands of meters on the ground, due to installation uncertainty and launch shift (Lin et al., 2018; Storey et al., 2014). It is also expected that the mounting coefficients will be fine-tuned before the end of commissioning using selected high accuracy, cloud-free ground control points derived from USGS Digital Orthophoto Quadrangle (DOQ) data (Kieffer et al., 2008; USGS, 2018) for SBG sensors, similar to those used for Landsat (Storey et al., 2014). A more accurate orthoimage dataset recently acquired by the US Department of Agriculture National Agriculture Imagery Program (NAIP) (Bresnahan, 2022; USDA, 2023) can also be used for such a purpose.

Long-term monitoring of geolocation accuracy assessment also uses the Global Land Survey (GLS) (Gutman et al., 2013; Rengarajan et al., 2015), in addition to regional USGS DOQ ground control points. If significant drifts occur, re-processing of data collections is required by applying temporal pointing variations (Storey et al., 2014; Lin et al., 2020; Lin et al., 2022). Landsat 8 has achieved geolocation accuracy of 18 meters of circular error at 90th percentile (CE90) (Storey et al., 2014) in data Landsat Collection 1. After Sentinel-2 from the ESA was launched in June 2015, a global reference image (GRI) database was generated (Clerc et al., 2021; Dechoz et al., 2015). The Landsat 7 GLS database was augmented with Landsat 8 data, which was further harmonized with GRI with space-based triangulation (Storey et al., 2019). Reprocessed Landsat collection 2 of Landsat 8 data has achieved geolocation accuracy of 8 meters at CE90 using GCPs from the harmonized GLS (Rengarajan et al., 2020). The accuracy is achieved by registering level-1 products to the control base of GRI and Landsat 8 augmented GLS (USGS, 2021).

The ground sampling distances (GSDs) for SBG are expected to be about 30 m and 60 m for the VSWIR sensor and TIR sensor, respectively. Sentinel-2 has three GSDs, 10, 20 and 60 m. Landsat 8 has GSDs at 30 m for visible, near-infrared, and short-wave infrared bands, 100 m for thermal bands, and 15 m for a panchromatic band. Because the GSDs for Landsat and Sentinel-2 are comparable to SBG, SBG (and collaborating missions CHIME, TRISHA, and LSTM) can

employ the same geometric calibration methods and achieve similar sub-pixel geolocation accuracy.

The geolocation accuracy assessment will include the effects from focal length deviation. If the focal length deviates from the nominal designed value, it should be corrected by putting the focal length as a geolocation parameter in a look-up table (Tilton et al., 2019; Seo et al., 2016; Wang, et al., 2014).

Geolocation calibration is a major part of instrument on-orbit geometric calibration and assessment. Other parts include MTF and BBR characterization. MTF and BBR calibration activities are performed in pre-launch tests (Knight & Kvaran, 2014; Lin et al., 2011) (See section 3). On-orbit MTF assessment may be performed using lunar observations (Choi et al., 2014; Wang et al., 2015), Earth surface target (Tilton et al., 2017a), or special setup on the ground (Wenny et al., 2015), see Table 6. On-orbit BBR assessment may be performed similarly using lunar observations (Wang et al., 2015) and Earth surface targets (Tilton et al., 2017b, 2019).

Note that instrument geolocation performance highly depends on the performance of spacecraft ephemeris (position and velocity) and attitude. Loss of pointing accuracy (LOPA) occurs during orbit management in drag make-up and inclination adjustment maneuvers and following these maneuvers. It is important to understand the impacts of these maneuvers on the quality of instrument data products. Therefore, the SBG CVWG recommends that a flight dynamic support team quantify the time span of any LOPA event and data product generation team withhold products during such a time span from releasing to users.

Table 6. *SBG CVWG Recommended CEOS Endorsed Global Sites for Geometric Calibration*

Site Name	Location
1 mi Road Grid	42°N, 96°W, extended
Baotou	40.8517°N, 109.6289°E
Big Spring	32.220436°N, 101.512524°W
Chesapeake Bay Bridge	37.034342°N, 76.079861°W
FGI Sjöckulla	60.2421°N, 24.3838°E
Jiaozhou Bay Bridge	36.152706°N, 120.221456°E
King Faud Causeway	26.1961°N, 50.342°E
Lake Pontchartrain	30.2125°N, 90.1219°W
Peng Hu	23.519989°N, 119.583581°E
Pueblo Range	38.2827°N, 104.6066°W
Salon de Provence	43.6061°N, 5.12°E
San Mateo Bridge	37.600958°N, 122.209033°W
Shadnagar	17.034249°N, 78.183060°E
Sioux Falls Range	43.555562°N, 96.745806°W
Stennis	30.3855°N, 89.6285°W
Suramadu Bridge	7.179025°S, 112.780693°E

Where all sites except the Pueblo Range and Sioux Falls Range sites listed above are also specifically recommended for Geometric, Spatial calibration.

When the SBG TIR instrument data are used in combination with the SBG VSWIR instrument data, the finer resolution VSWIR data will be re-sampled to the coarser resolution TIR location. The re-sampler will be designed such that the MTF of the re-sampled VSWIR data are compatible with the MTF of the TIR data. Similar re-sampler(s) should be designed to combine other instrument data for higher level downstream data product generation.

5.4.2 Aquatic Targets

To support remote sensing of coastal and inland aquatic waters, a number of calibration and validation resources are used for accurately calibrating the TOA satellite observations. In addition to lakes mentioned under terrestrial targets (section 5.4.1.2), additional networks and measurements across the open ocean help to facilitate thermal calibration. The non-thermal sites in Table 7 can be used for validation of surface radiometry from orbit or SVC, including the Marine Optical BuoY (MOBY; Clark, D. K., et al., 2002), BOUSSOLE (Antoine et al., 2008), WATERHYPERNET (<https://waterhypernet.org/>), and the Aerosol Robotic Network - Ocean Color (AERONET-OC; Zibordi et al, 2009). MOBY and BOUSSOLE are currently used primarily for SVC, with MarONet and EURYBIA coming on line in the next few years. Because of its extreme clarity and hence ease to model, the South Pacific Gyre has also been used occasionally for SVC when matches with *in situ* measurements are few in number (Zibordi & Mélin, 2017), such as during the first months of a mission. For aquatic remote sensing at visible wavelengths, SVC with buoy and platform (or similar asset) addresses transfer-to-orbit changes in pre-launch calibration, pre-launch calibration to aquatic target uncertainties and biases in surface radiometry stemming from the atmospheric correction (Antoine et al., 2008; Clark et al., 1997; Clark, D. K., et al., 2002; Vansteenwegen et al., 2019; Zibordi et al., 2009). As previously mentioned, because atmospheric correction biases are also addressed, SVC optimizes only the accuracy of water leaving radiance, not at-sensor radiance.

Table 7. Global Instrumented Aquatic Sites for *Vicarious* Calibration

Site name	Location
Aqua Alta	45.3142°N, 12.5083°E
Bahia Blanca	39.148°S, 61.722°W
Casablanca Platform	40.717°N, 1.358°E
Chesapeake Bay	39.124°N, 76.349°W
Galata Platform	43.045°N, 28.193°E
Kemigawa Offshore	35.611°N, 140.023°E
Lake Okeechobee N	27.139°N, 80.789°W
Lake Tahoe	39.0°N, 120.0°W
LISCO	40.955°N, 73.342°W
Lucinda	18.520°S, 146.386°E
Oostende	14.7833°N, 2.9194°E
Palgrunden	58.755°N, 13.152°E
Salton Sea	33.22532°N, 115.82425°W
San Marco Platform	2.942°S, 40.215°E

Section-7 Platform	44.546°N, 29.447°E
Socheongcho	37.423°N, 124.738°E
USC SeaPRISM	33.564°N, 118.118°W
Venise	45.314°N, 12.508°E
WaveCIS Site CSI 6	28.867°N, 90.483°W
Zeebrugge-MOW1	51.362°N, 3.120°E
MOBY 272*	20.4322°N, 157.0936°W
BOUSSOLE*	43.367°N, 7.900°E
MarONet*	TBD Near Perth
EURYBIA*	TBD Mediterranean Sea

*Sites designated for system vicarious calibration.

MOBY (<https://mlml.sjsu.edu/moby/>) is a primary radiometry resource used for validation and SVC of ocean color sensors since the launch of NASA's Sea-viewing Wide Field-of-view Sensor (SeaWiFS) and has been in continuous operation since 1997. MOBY is moored off the island of Lanai, Hawai'i and is an autonomous optical buoy measuring daily near real time upwelling radiance (L_u) from 340-955 nm at approximately 1, 5, and 9 m depth and downwelling irradiance (E_d) from underwater at these depths and at the surface. Progress is underway to augment MOBY with MOBY-like enhanced technology buoy systems with a broader global distribution. Additional planned sites include MarONet at the Australian site off the coast of Perth and the European Radiometry Buoy and Infrastructure (EURYBIA) for the Copernicus site near Lampedusa Island in the Mediterranean Sea (Liberti et al., 2020).

The BOUSSOLE buoy (<http://www.obs-vlfr.fr/Boussole/html/project/introduction.php>) is deployed in the Ligurian Sea (Mediterranean Sea) off of Nice, France. Radiometer measurements of irradiance are made at 4.5 m above the water surface (E_s) and downwelling irradiance, upwelling irradiance (E_u), and upwelling radiance are made at 4 and 9 m depths. Data are collected every 15 min during daylight and hourly at night. There were operational sequences of data collection beginning in 2002 and nearly uninterrupted data collections since 2005.

WATERHYPERNET (<https://waterhypernet.org/>) is a hyperspectral radiometer system (350-900 nm) network that has had prototypes deployed on a platform in the Adriatic Sea since 2018 and operating autonomously since 2019. There are three additional sites operating the system on platforms in Belgium: Aqua Alta, Oostende, and Blankart. Production level systems are planned for deployment at a large variety of coastal and inland water sites. At each station, downwelling irradiance, downwelling sky radiance (L_d) and upwelling radiance measurements are made automatically with the radiometer. LANDHYPERNET deployments of instruments, which is a terrestrial version of the WATERHYPERNET program, both now falling under the moniker HYPERNET-EU. SBG will be working to extend this network into the USA as part of a calibration/validation infrastructure for the mission. The SBG project is exploring setting up stations in the Mid-Atlantic and West Coast regions of the USA, an effort that is currently being spearheaded by Turpie.

AERONET-OC (https://aeronet.gsfc.nasa.gov/new_web/ocean_color.html) is a network of above water multispectral radiometer measurement systems called the SeaWiFS Photometer Revision for Incident Surface Measurements (SeaPRISM), which are on fixed platforms augmenting the

globally distributed network of Sun photometers of AERONET. There have been 38 systems installed (or moved) globally since the initial installations in 2009 and 15 of these serviced systems are operating. The SeaPRISM measures Sun irradiance, sky radiance (L_i), and total radiance from the sea (L_T) every 30 s at ocean color algorithm channels from 400 to 1,020 nm. The system is designed not to collect data when clouds are obscuring the Sun. Derived normalized water-leaving radiance of the site-specific seawater apparent water properties are provided.

6 Summary

In this paper, we considered high-level calibration and validation concepts that are relevant to the SBG mission formulation, with a heavy focus on calibration and surface radiometry. In general, the SBG project has the opportunity to work with all collaborating agencies to use common metrological and radiometric language with terms derived from international standards and use common techniques for pre-launch characterization and calibration; use and share reference sources; use common match-up datasets, reference data sets, and calibration and validation methods; and use open, standard algorithms for on-orbit calibration and validation and generation of at-sensor and surface radiometry. In particular, the current recommended data set for solar spectral irradiance is the TSIS-1 Hybrid Solar Reference Spectrum (Coddington et al., 2021, 2023) for solar calibration and generation of all reflectance data products. The SBG project should leverage the calibration and validation experiences of the current and upcoming missions mentioned in the introduction of this paper, including the USA missions EMIT, PACE and GLIMR given their greater accessibility.

SBG should keep as much information and steps in common as possible in support of a suite of standard data products across missions. To that end, it is further recommended that all collaborating space agencies have advanced discussions and agreements regarding work-flows, modes of communication and conflict resolution necessary for effective collaboration towards these common resources. To support data harmonization and interoperability of science data products, the SBG CVWG recommended that this includes transformation of science data products onto common spatial and spectral grids and the use of ISO data standard or CEOS protocols for development of ARD (however, spectral reflectance should be made available without aggregation). It is also recommended that a calibration and validation infrastructure be established, including the development of computational infrastructure and open-source analysis tools for comparing SBG imaging spectroscopy or thermal infrared imagery with data sets from other surface, airborne, or spaceborne sensors, as provided by collaborating agencies.

To benefit from data harmonization of multiple missions, inter-calibration needs to be a strategic priority. Orbital simulations for SBG VSWIR and TIR instruments underscore that orbital altitude, imaging revisit frequencies, imaging swath width of existing and planned space architectures for Earth imaging suggest more synergistic cooperation around designed SNO or NSO opportunities is needed. In addition, there are clear geographic imaging patterns for SNO and NSO that may not align very well with current ground-based radiometric calibration reference sites, placing a greater emphasis on expanding vicarious calibration networks or campaigns and on-board or celestial references. The SBG CVWG recommends strong mission

cooperation between USA and international space agencies to optimize orbits in support of inter-calibration and higher quality terrestrial remote sensing science and application data products.

For on-orbit long-term monitoring and time-dependent, inter-calibration, lunar calibration is recommended because only the Moon could be used as a common calibration reference free of effects from the Earth's atmosphere. But use of the Moon depends on the removal of current biases in lunar spectral irradiance predictions. A mission concept should plan on frequent lunar observations during commissioning, then at least once a month for a year, then becoming spaced out; also, soon after any anomalous event in orbit. This includes any provisions that must be made in spacecraft design, accurate pointing and pointing knowledge, accurate and detailed knowledge of the instrument spatial response, instrument temperature control, and mission concept of operations. Using solar calibration is also highly recommended to provide continuous monitoring throughout the mission, especially if the instrument design includes multiple detectors for the same band.

For inter-calibration, it is always best to match the measurements in as close as possible spectral range, spatial coverage, viewing and illumination geometry, and time window. At the beginning of the mission, the matching criteria may be expanded slightly to obtain more data points for comparison. As the mission continues, the matching criteria can be narrowed again to improve data quality (BIPM et al., 2008; Wielicki et al., 2008) in both forward-processing and reprocessing.

Validation determines whether threshold uncertainty targets are actually being met by comparing SBG satellite data products against measurements made *in situ*. The validation strategy must develop a surface sampling strategy that addresses temporal and spatial variability of the geophysical property being vetted against actual surface measurements. This may include airborne platforms to better spatially integrate surface observations to scales commensurate with satellite observations. It is also ideal that validation strategy assures that the *in situ* measurement uncertainty (or some aggregate) to be much less than the quality threshold uncertainty to ensure meaningful results. In general, the SBG CVWG recommends that the NASA SBG project and collaborating agencies should choose or define methods and protocols for selecting and archiving validation and vicarious calibration match-ups between *in situ* and satellite measurements.

To facilitate this development for science data products, input will be needed from the algorithm and application developers regarding the expected value, valid range, and spatial and temporal variation for each geophysical quantity identified to be produced by the SBG mission, especially any standard data products across agencies. Spatial and temporal variability must be quantified at global, scene, and subpixel scales. Observing System Simulation Experiments (OSSE) results may also help to fill in knowledge gaps in the information provided by the community or literature.

The SBG CVWG also noted that future calibration and validation plans will continue to get additional input from the algorithm and application communities regarding resources available to acquire *in situ* data, e.g., measurement networks; observation stations, towers, and buoys; airborne campaigns, cruises, and field campaigns, including efforts employing unmanned vehicles. Any SBG validation plan should draw on any existing validation protocols or studies undertaken by algorithm developers or end users in these communities, or protocols and

standards accepted by international working groups. Processing infrastructure common to both validation and vicarious calibration includes, but is not limited to, ground processing software for extracting matching satellite data and capability to process surface data.

The SBG CVWG finally recommends that the NASA SBG project and its collaborating agencies identify or develop joint surface measurement networks. Instrumented terrestrial and aquatic networks of sites for radiometric, thermal, spectral, and geometric calibration are critical to the generation of high-quality science data products. Likewise, arrays of surface instruments are necessary for collection of a large sample of validation data. This paper has touched on a sizable sample of potential resources; however, with a planned launch of SBG in 2028, it remains unclear what portion of existing resources will be available when the SBG mission is in orbit. The project will need to track these resources and must be prepared to support their maintenance to ensure adequate surface data are available for calibration, validation, and algorithm development.

Data Availability Statement

For the simultaneous and near-simultaneous calibration opportunity analysis, a 0.2° grid and northern hemisphere spring equinox temporal scenarios were used. Orbit parameters were derived from Earth observation mission sources as follows: Landsat 8 - Irons et al., 2012 and Roy et al., 2014; Sentinel-2a - Drusch et al., 2012; CHIME – ESA-EOPSM-CHIM-MRD-3216, 2021; PACE – Werdell et al., 2019; LSTM – ESA-EOPSM-HSTR-MRD-3276, 2021; **CLARREO-Pathfinder – Shea et al., 2020**. Earth observation mission orbital characteristics can also be centrally accessed from Ramasari Chandra, et al., 2022 and <https://calval.cr.usgs.gov/apps/compendium>. Orbital simulations were done via Systems ToolKit™ software (<https://www.ansys.com/products/missions/ansys-stk>) and can be done with similar tools (e.g. <https://ncc.nesdis.noaa.gov/VIIRS/SNOPredictions/>). Total Solar Irradiance Sensor (TSIS)-1 Hybrid Solar Reference Spectrum (HSRS), Version 2, by Coddington et al 2023, published by the Laboratory for Atmospheric and Space Physics is found at https://lasp.colorado.edu/lisird/data/tsis1_hsrs_p1nm.

Acknowledgements

The authors would like to acknowledge and thank the many proponents who supported precursor studies like the Hyperspectral Infrared Imager (HypIRI) campaign. Authors KRT, KAC, CJC, LSG, HK, GL, AKS, CA, RK, and SNRC contributed a significant amount of effort and material in preparing this paper, the other authors participated in working group discussion and contributed intellectually to analyses and material presented. We note particularly the modeling, results and text provided by AC and SNRC for section 4 of this paper. The authors thank the SBG Calibration and Validation Working Group, including >106 experts at government and private institutions within and outside of the USA, for their participation in lengthy discussions, recommendations and presenting material relevant to this manuscript. In particular we acknowledge and are grateful for input from Dr. Robert E. Wolfe (NASA/GSFC) regarding geometric calibration and Dr. Glynn Hulley (NASA/JPL) regarding thermal calibration. Additionally, the authors thank the NASA Program Managers: Woody Turner, Benjamin Phillips, and Laura Lorenzoni, for their guidance and leadership over the course of Cal/Val concept development for SBG. Part of the research described in this paper was carried out at the

United States Geological Survey. Government sponsorship acknowledged. Any use of trade, product, or firm names is for descriptive purposes only and does not imply endorsement by the U.S. Government. We gratefully acknowledge the service provided by the editors and two anonymous reviewers which subsequently led to an improved manuscript.

References

- Ahtee, V., Brown, S. W., Larason, T. C., Lykke, K. R., Ikonen, E., & Noorma, M. (2007). Comparison of absolute spectral irradiance responsivity measurement techniques using wavelength-tunable lasers. *Applied Optics*, 46, 4228-4236. <https://doi.org/10.1364/AO.46.004228>
- Alonso, K., Bachmann, M., Burch, K., Carmona, E., Cerra, D., De los Reyes, R., et al. (2019). Data products, quality and validation of the DLR Earth sensing imaging spectrometer (DESI). *Sensors*, 19(20), 4471. <https://doi.org/10.3390/s19204471>
- Anderson, G. P., Berk, A., Acharya, P. K., Matthew, M. W., Bernstein, L. S., Chetwynd Jr., J. H., et al. (2000). MODTRAN4: Radiative transfer modeling for remote sensing. *Proc. SPIE*, 4049, 176-183. <https://doi.org/10.1117/12.410338>
- Angal, A., McCorkel, J., & Thome, K. (2016). Evaluation of GLAMR-based calibration for SI-traceable field reflectance retrievals. *SPIE Proceedings, Earth Observing Systems XXI*, 9972, 554-559. <https://doi.org/10.1117/12.2238630>
- Antoine, D., Guevel, P., Deste, J.-F., Becu, G., Louis, F., Scott, A. J., & Bardey, P. (2008). The “BOUSSOLE” buoy—A new transparent-to-swell taut mooring dedicated to marine optics: Design, tests, and performance at sea. *Journal of Atmospheric and Oceanic Technology*, 25, 968-989. <https://doi.org/10.1175/2007JTECHO563.1>
- Barnes, R., Brown, S. W., Lykke, K. R., Guenther, B., Schwarting, T., Turpie, K.R., et al. (2015). Comparison of two methodologies for calibrating satellite instruments in the visible and near infrared. *Applied Optics*, 54(35), 10376–10396. <https://doi.org/10.1364/AO.54.010376>
- Barnsley, M., Settle, J., Cutter, M., Lobb, D., & Teston, F. (2004). The PROBA/CHRIS mission: A low-cost smallsat for hyperspectral multiangle observations of the Earth surface and atmosphere. *IEEE Trans. Geosci. Remote Sens.* 42, 1512–1520. <https://doi.org/10.1109/TGRS.2004.827260>
- Barsi, J. A., Markham, B. L., McCorkel, J. T., McAndrew, B., Donley, E., Morland, E., et al. (2019). The Operational Land Imager-2: Prelaunch spectral characterization. *SPIE Proceedings, Earth Observing Systems XXIV*. <https://doi.org/10.1117/12.2529776>
- Bilimoria, K. D., & Krieger, R. A. (2011). Slot architecture for separating satellites in sun-synchronous orbits. *AIAA SPACE 2011 Conference & Exposition*. <https://doi.org/10.2514/6.2011-7184>
- BIPM, I., IFCC, I., ISO, I., & IUPAP, O. (2008). Evaluation of measurement data - Guide to the expression of uncertainty in measurement (GUM 1995 with minor corrections). Joint Committee

for Guides in Metrology, JCGM, 100:2008. Available at <https://www.bipm.org/en/committees/jc/jcgm/publications>

Bouvet, M., Thome, K., Berthelot, B., Bialek, A., Czapla-Myers, J., Fox, N. P., et al. (2019). RadCalNet: A radiometric calibration network for Earth observing imagers operating in the visible to shortwave infrared spectral range. *Remote Sensing*, 11(20), 2401. <https://doi.org/10.3390/rs11202401>

Brell, M., Guanter, L., Segl, K., Scheffler, D., Bohn, N., Bracher, A., et al. (2021). The EnMAP satellite – Data product validation activities. *2021 11th Workshop on Hyperspectral Imaging and Signal Processing: Evolution in Remote Sensing (WHISPERS)*. IEEE. Amsterdam, Netherlands, 2021, pp. 1-5. <https://doi.org/10.1109/WHISPERS52202.2021.9484000>

Bresnahan, P. (2022). NAIP Geolocation Accuracy Assessment. Available online: https://view.officeapps.live.com/op/view.aspx?src=https%3A%2F%2Fcalval.cr.usgs.gov%2Fapps%2Fsites%2Fdefault%2Ffiles%2Fjacie%2F2022-S2-Paul_Bresnahan_NAIP_Geolocation_Accuracy_Assessment.pptx&wdOrigin=BROWSELINK (last accessed 25 January 2023)

Brown, S. W., Eppeldauer, G. P., & Lykke, K. R., (2006). Facility for spectral irradiance and radiance responsivity calibrations using uniform sources. *Applied Optics*, 45, 8218-8237. <https://doi.org/10.1364/AO.45.008218>

Cao, C., & Heidinger, A.K. (2002). Intercomparison of the longwave infrared channels of MODIS and AVHRR/NOAA-16 using simultaneous nadir observations at orbit intersections. In Earth Observing Systems VII, William L. Barnes (editor), *Proceedings of SPIE*, 4814, 306-316. <https://doi.org/10.1117/12.451690>

Cao, C., Weinreb, M., & Xu, H. (2004). Predicting simultaneous nadir overpasses among polar-orbiting meteorological satellites for the intersatellite calibration of radiometers. *Journal of Atmospheric and Oceanic Technology*, 21(4), 537-542. [https://doi.org/10.1175/1520-0426\(2004\)021%3C0537:PSNOAP%3E2.0.CO;2](https://doi.org/10.1175/1520-0426(2004)021%3C0537:PSNOAP%3E2.0.CO;2)

Cao, C., Xu, H., Sullivan, J., Mcmillin, L., Ciren, P., & Hou, Y. (2005). Intersatellite radiance biases for the High Resolution Infrared Radiation Sounders (HIRS) on-board NOAA-15, -16, and -17 from simultaneous nadir observations. *Journal of Atmospheric and Oceanic Technology*, 22, 381-395. <https://doi.org/10.1175/JTECH1713.1>

Celesti, M., Rast, M., Adams, J., Boccia, V., Gascon, F., Isola, C., & Nieke, J. (2022). The Copernicus Hyperspectral Imaging Mission for the Environment (CHIME): Status and planning. *IGARSS 2022-2022 IEEE International Geoscience and Remote Sensing Symposium* (pp. 5011-5014). <https://doi.org/10.1109/IGARSS46834.2022.9883592>

Chander, G., Hewison, T. J., Fox, N., Wu, X., Xiong, X., & Blackwell, W. J. (2013). Overview of intercalibration of satellite instruments. *IEEE Transactions on Geoscience and Remote Sensing*, 51(3), 1056-1080.

Chapman, J. W., Thompson, D. R., Helmlinger, M. C., Bue, B. D., Green, R. O., Eastwood, M. L., et al. (2019). Spectral and radiometric calibration of the next generation airborne visible infrared spectrometer (AVIRIS-NG). *Remote Sensing*, 11(18), 2129. <https://doi.org/10.3390/rs11182129>

Choi, T., Xiong, X., & Wang, Z. (2014). On-orbit lunar modulation transfer function measurements for the Moderate Resolution Imaging Spectroradiometer, *IEEE Transactions on Geoscience and Remote Sensing*, 52(1), 270-277. <https://doi.org/10.1109/TGRS.2013.2238545>

Choi, T., Cao, C., Shao, X., & Wang, W. (2022). S-NPP VIIRS Lunar Calibrations over 10 Years in Reflective Solar Bands (RSB). *Remote Sensing*, 14(14), 3367.

Clark, D. K., Gordon, H. R., Voss, K. J., Ge, Y., Broenkow, W., & Trees C. (1997). Validation of atmospheric correction over the oceans. *Journal of Geophysical Research: Atmospheres*, 102(D14), 17209-17217. <https://doi.org/10.1029/96JD03345>

Clark, D. K., Yarbrough, M. A., Feinholz, M. E., Flora, S., Broenkow, W., Kim, Y. S., Johnson, B. C., et al. (2002). MOBY, a radiometric buoy for performance monitoring and vicarious calibration of satellite ocean color sensors: Measurement and data analysis protocols. *Ocean Optics Protocols for Satellite Ocean Color Sensor Validation, Revision 3, Volume 2*. J. L. Mueller and G. S. Fargion, Eds. Greenbelt, MD, NASA Goddard Space Flight Center. NASA/TM--2002-21004:138-170.

Clark, R. N., Swayze, G. A., Livo, K. E., Kokaly, R. F., King, T. V., Dalton, J. B., et al. (2002). Surface reflectance calibration of terrestrial imaging spectroscopy data: A tutorial using AVIRIS. In *Proceedings of the 10th Airborne Earth Science Workshop* (Vol. 2). Pasadena, CA, USA: Jet Propulsion Laboratory.

Clerc, S., Van Malle, M.N., Massera, S., Quang, C., Chambrelan, A., Guyot, F., et al. (2021). Copernicus SENTINEL-2 geometric calibration status, *IEEE International Geoscience and Remote Sensing Symposium*, pp. 8170-8172. <https://doi.org/10.1109/IGARSS47720.2021.9555090>

Cocks, T., Jenssen, R., Stewart, A., Wilson, I., & Shields, T. (1998). The HyMap airborne hyperspectral sensor: The system, calibration and performance. *European Association of Remote Sensing Laboratories (EARSeL) Workshop on Imaging Spectroscopy*, Zurich, October 6–8, 1998, Extended Abstracts, p. 37–43.

Coddington, O., Lean, J., Pilewskie, P., Snow, M., Richard, E., Kopp, G., et al. (2019). Solar irradiance variability: Comparisons of models and measurements. *Earth and Space Science*, 6, 2525-2555. <https://doi.org/10.1029/2019EA000693>

Coddington, O. M., Richard, E. C., Harber, D., Pilewskie, P., Woods, T.N., Chance, K., et al. (2021). The TSIS-1 Hybrid Solar Reference Spectrum. *Geophysical Research Letters*, 48, e2020GL091709. <https://doi.org/10.1029/2020GL091709>

Coddington, O. M., Richard, E. C., Harber, D., Pilewskie, P., Woods, T. N., Snow, M., Chance, K., Liu, X., & Sun, K. (2023). Version 2 of the TSIS-1 Hybrid Solar Reference Spectrum and

Extension to the Full Spectrum. *Earth and Space Science*. Accepted advanced online publication.
<https://doi.org/10.1029/2022EA002637>

Coll, C., Wan, Z., & Galve, J. M. (2009). Temperature-based and radiance-based validations of the V5 MODIS land surface temperature product. *J. Geophys. Res.*, 114, D20102.
<https://doi.org/10.1029/2009JD012038>

Coppo, P., Taiti, A., Pettinato, L., Francois, M., Taccola, M., & Drusch, M. (2017). Fluorescence imaging spectrometer (FLORIS) for ESA FLEX mission. *Remote Sensing*, 9(7), 649.
<https://doi.org/10.3390/rs9070649>

Cosnefroy, H., Leroy, M., & Briottet, X., (1996). Selection and characterization of Saharan and Arabian desert sites for the calibration of optical satellite sensors. *Remote Sensing of Environment*, 58(1), 101-114. [https://doi.org/10.1016/0034-4257\(95\)00211-1](https://doi.org/10.1016/0034-4257(95)00211-1)

Czajkowski, K. P., Goward, S. N., Stadler, S. J., & Walz, A. (2000). Thermal remote sensing of near surface environmental variables: Application over the Oklahoma Mesonet, *The Professional Geographer*, 52(2), 345-357. <https://doi.org/10.1111/0033-0124.00230>

Czapla-Myers, J., Thome, K., Wenny, B., & Anderson, N. (2020). Railroad Valley radiometric calibration test site (RadCaTS) as part of a global radiometric calibration network (RadCalNet)," *IGARSS 2020 - 2020 IEEE International Geoscience and Remote Sensing Symposium, 2020*, pp. 6413-6416. <https://doi.org/10.1109/IGARSS39084.2020.9323665>

Datla, R. U., Rice, J. P., Lykke, K. R., Johnson, B. C., Butler, J. J., & Xiong, X. (2011). Best practice guidelines for pre-launch characterization and calibration of instruments for passive optical remote sensing. *Journal of Research of the National Institute of Standards and Technology*, 116(2), 621. <https://doi.org/10.6028/jres.116.009>

Dechoz, C., Poulain, V., Massera, S., Languille, F., Greslou, D., de Lussy, F., et al. (2015). Sentinel 2 global reference image. *Image and Signal Processing for Remote Sensing XXI*. Proc. SPIE, 9643, 96430A. <https://doi.org/10.1117/12.2195046>

Dollfus, A. (1962). The Polarization of Moonlight. In Z. Kopal and K. Mikhailov (Eds.), *Physics and Astronomy of the Moon* (pp. 131-159). New York and London: Academic Press.

Drusch, M., Del Bello, U., Carlier, S., Colin, O., Fernandez, V., Gascon, F., Hoersch, B. et al. (2012). Sentinel-2: ESA's optical high-resolution mission for GMES operational services. *Remote Sensing of Environment*, 120, 25-36. <https://doi.org/10.1016/j.rse.2011.11.026>

Durell, C. (2019). IEEE P4001 hyperspectral standard: Progress and cooperation. *IGARSS 2019 - 2019 IEEE International Geoscience and Remote Sensing Symposium*, 4432-4434.
<https://doi.org/10.1109/IGARSS.2019.8900295>

Durell, C., & Russell, B. (2020). On demand vicarious calibration for analysis ready data: The FLARE Network. *Proceedings of 34th Annual Small Satellite Conference. SSC20-S1-01*.
<https://digitalcommons.usu.edu/smallsat/2020/all2020/177/>

Dwyer, J. L., Roy, D. P., Sauer, B., Jenkerson, C. B., Zhang, H. K., & Lymburner, L. (2018). Analysis ready data: Enabling analysis of the Landsat archive. *Remote Sensing*, 10(9), 1363.
<https://doi.org/10.3390/rs10091363>

Eplee Jr, R. E., Bailey, S. W., Barnes, R. A., Kieffer, H. H., & McClain, C. R. (2006, September). Comparison of SeaWiFS on-orbit lunar and vicarious calibrations. In *Earth Observing Systems XI* (Vol. 6296, pp. 336-342). SPIE.

Eplee Jr, R. E., Meister, G., Patt, F. S., Turpie, K. R., Bailey, S. W., & Franz, B. A. (2019). The NASA OBP 2020 on-orbit calibration of SNPP VIIRS for ocean color applications. In *Earth Observing Systems XXIV* (Vol. 11127, pp. 254-272). SPIE.

European Space Agency, Earth and Mission Science Division (2021) Copernicus High Spatio-Temporal Resolution Land Surface Temperature Mission: Mission Requirements Document, ESA-EOPSM-HSTR-MRD-3276, Revision 3,
https://esamultimedia.esa.int/docs/EarthObservation/Copernicus_LSTM_MRD_v3.0_Issued_20210514.pdf

European Space Agency, Earth and Mission Science Division (2021) Copernicus Hyperspectral Imaging Mission for the Environment – Mission Requirements Document, ESA-EOPSM-CHIM-MRD-3216, Revision 3,
https://esamultimedia.esa.int/docs/EarthObservation/Copernicus_CHIME_MRD_v3.0_Issued_21_01_2021.pdf

Feingersh, T., & Ben-Dor, E. (2015). SHALOM—A commercial hyperspectral space mission. In Shen-En Qian (Ed.), *Optical payloads for space missions* (pp. 247-262).
<https://doi.org/10.1002/9781118945179.ch11>

Ferrero, C. (2009). *Vocabulaire international des termes fondamentaux et généraux de métrologie (VIM)*. Presented at Instituto Nazionale di Ricerca Metrologica (INRIM), Tunis, Tunisia. <https://doi.org/10.13140/RG.2.1.3771.4320>

Fulbright, J., Lei, N., Efremova, B., Xiong, X. (2015) Suomi-NPP VIIRS Solar Diffuser Stability Monitor Performance, *IEEE Transactions on Geoscience and Remote Sensing*, 54(2), 631-639.
<https://doi.org/10.1109/TGRS.2015.2441558>

Gil, J., Rodrigo, J. F., Salvador, P., Gómez, D., Sanz, J., & Casanova, J.L. (2020). An empirical radiometric intercomparison methodology based on global simultaneous nadir overpasses applied to Landsat 8 and Sentinel-2, *Remote Sensing*, 12, 2736.
<https://doi.org/10.3390/rs12172736>

Green, R. O., Eastwood, M. L., Sarture, C. M., Chrien, T. G., Aronsson, M., Chippendale, B. J., et al. (1998). Imaging spectroscopy and the Airborne Visible/InfraRed Imaging Spectrometer (AVIRIS). *Remote Sensing of Environment*, 65(3), 227-248. [https://doi.org/10.1016/S0034-4257\(98\)00064-9](https://doi.org/10.1016/S0034-4257(98)00064-9)

Green, R. O., Mahowald, N., Ung, C., Thompson, D. R., Bator, L., Bennet, M., et al. (2020). The Earth surface mineral dust source investigation: An Earth science imaging spectroscopy mission. In *2020 IEEE Aerospace Conference* (pp. 1-15).. <https://doi.org/10.1109/AERO47225.2020.9172731>

Green, R. O., Pavri, B. E., & Chrien, T.G. (2003). On-orbit radiometric and spectral calibration characteristics of EO-1 Hyperion derived with an underflight of AVIRIS and in situ measurements at Salar de Arizaro, Argentina. *IEEE Transactions on Geoscience and Remote Sensing*, 41(6), 1194-1203. doi: 10.1109/TGRS.2003.813204

Guanter, L., Kaufmann, H., Segl, K., Foerster, S., Rogass, C., Chabrillat, S., et al. (2015). The EnMAP spaceborne imaging spectroscopy mission for earth observation. *Remote Sensing*, 7(7), 8830-8857. <https://doi.org/10.3390/rs70708830>

GuilleVIC, P., Göttsche, F., Nickeson, J., Hulley, G., Ghent, D., Yu, Y., et al. (2018). Land surface temperature product validation best practice protocol. Version 1.1. In P. GuilleVIC, F. Göttsche, J. Nickeson & M. Román (Eds.), *Good Practices for Satellite-Derived Land Product Validation* (p. 58): Land Product Validation Subgroup (WGCV/CEOS), <https://doi.org/10.5067/doc/ceoswgcv/lpv/1st.001>

Gutman, G., Huang, C., & Chander, G. (2013). Assessment of the NASA-USGS Global Land Survey (GLS) datasets. *Remote Sensing of Environment* 134, 249–265. <https://doi.org/10.1016/j.rse.2013.02.026>

Hall, D. K., Box, J. E., Casey, K. A., Hook, S. J., Shuman, C. A., & Steffen, K. (2008). Comparison of satellite-derived and in-situ observations of ice and snow surface temperatures over Greenland. *Remote Sensing of Environment*, 112(10), 3739-3749, <https://doi.org/10.1016/j.rse.2008.05.007>

Helder, D., Markham, B., Morfitt, R., Storey, J., Barsi, J., Gascon, F., et al. (2018). Observations and recommendations for the calibration of Landsat 8 OLI and Sentinel 2 MSI for improved data interoperability. *Remote Sensing*, 10(9), 1340. <https://doi.org/10.3390/rs10091340>

Helder, D., Thome, K. J., Mishra, N., Chander, G., Xiong, X., Angal, A., & Choi, T. (2013). Absolute radiometric calibration of Landsat using a pseudo invariant calibration site. *IEEE Transactions on Geoscience and Remote Sensing*, 51(3), 1360-1369. <https://doi.org/10.1109/TGRS.2013.2243738>

Holben B. N., Eck, T. F., Slutsker, I., Tanre, D., Buis, J. P., Setzer, A., et al. (1998). AERONET - A federated instrument network and data archive for aerosol characterization. *Remote Sensing of Environment*, 66, 1-16. [https://doi.org/10.1016/S0034-4257\(98\)00031-5](https://doi.org/10.1016/S0034-4257(98)00031-5)

Hook, S. J., Cawse-Nicholson, K., Barsi, J., Radocinski, R., Hulley, G., Johnson, W., et al. (2020). In-flight validation of the ECOSTRESS, Landsats 7 and 8 thermal infrared spectral channels using the Lake Tahoe CA/NV and Salton Sea CA automated validation sites. *IEEE Transactions on Geoscience Remote Sensing*, 58(2), 1294-1302. <https://doi.org/10.1109/TGRS.2019.2945701>

Hook, S. J., Vaughan, R. G., Tonooka, H., & Schladow S.G. (2007). Absolute radiometric in-flight validation of mid infrared and thermal infrared data from ASTER and MODIS on the Terra spacecraft using the Lake Tahoe, CA/NV, USA, automated validation site. *IEEE Transactions on Geoscience and Remote Sensing*, 45(6), 1798-1807. <https://doi.org/10.1109/TGRS.2007.894564>

Irons, J. R., Dwyer, J. L., & Barsi, J. A. (2012). The next Landsat satellite: The Landsat data continuity mission. *Remote Sensing of Environment*, 122, 11-21. <https://doi.org/10.1016/j.rse.2011.08.026>

Hulley, G. C., Göttsche, F. M., Rivera, G., Hook, S. J., Freepartner, R.J., Martin, M.A., et al. (2021). Validation and quality assessment of the ECOSTRESS level-2 land surface temperature and emissivity product. *IEEE Transactions on Geoscience and Remote Sensing*, 60, 1-23. <https://doi.org/10.1109/TGRS.2021.3079879>

Iwasaki, A., Ohgi, N., Tanii, J., Kawashima, T., & Inada, H. (2011). Hyperspectral Imager Suite (HISUI)-Japanese hyper-multi spectral radiometer. In *2011 IEEE International Geoscience and Remote Sensing Symposium* (pp. 1025-1028). IEEE. <https://doi.org/10.1109/IGARSS.2011.6049308>

Khakurel, P., Leigh, L., Kaewmanee, M., & Teixeira Pinto, C. (2021). Extended pseudo invariant calibration site-based trend-to-trend cross-calibration of optical satellite sensors. *Remote Sensing*, 13(8). 1545. doi:10.3390/rs13081545

Kieffer, H. H. (1997). Photometric stability of the lunar surface. *Icarus*, 130, 323–327. <https://doi.org/10.1006/icar.1997.5822>

Kieffer, H. (2021a). Advances in the SLIM lunar spectral irradiance model: Many observations, one Moon. In *CALCON 2021 Proceedings, Logan, UT. Conference on Characterization and Calibration for Remote Sensing*. <https://digitalcommons.usu.edu/calcon/CALCON2021/all2021content/23>

Kieffer, H. (2021b). Status of the SLIMED model; converging on the real Moon. In *GSICS VIS/NIR Web Meeting for August 2021. Global Space-based Inter-Calibration System*. http://gsics.atmos.umd.edu/pub/Development/20210812/Kieffer_21octGVN.pdf

Kieffer, H. (2022). Multiple instrument based spectral irradiance of the Moon. *Journal of Applied Remote Sensing*. 16(3). <https://doi.org/10.1117/1.JRS.16.038502>

Kieffer, H. H., & Stone, T. C. (2005). The spectral irradiance of the Moon. *Astron. Jour.*, 129, 2887–2901. <https://doi.org/10.1086/430185>

Kieffer, H. H., Mullins, K. F., & MacKinnon, D. J., (2008). Validation of the ASTER instrument Level 1A scene geometry. *Photogrammetric Engineering & Remote Sensing*, 74(3), 289-301. <https://doi.org/10.14358/PERS.74.3.289> [Data files available from USGS EROS]

Knight, E., & Kvaran, G. (2014). Landsat-8 Operational Land Imager design, characterization and performance, *Remote Sens.*, 6(11), 10286-10305. <https://doi.org/10.3390/rs61110286>

Krutz, D., Müller, R., Knodt, U., Günther, B., Walter, I., Sebastian, I., et al. (2019). The instrument design of the DLR earth sensing imaging spectrometer (DESI). *Sensors*, 19(7), 1622. <https://doi.org/10.3390/s19071622>

Kuhlmann, G., Hueni, A., Damm, A., & Brunner, D. (2016). An algorithm for in-flight spectral calibration of imaging spectrometers. *Remote Sensing*, 8(12), 1017. <https://doi.org/10.3390/rs8121017>

Lean, J. L., Coddington, O., Marchenko, S.V., Machol, J., DeLand, M.T., & Kopp, G. (2020). Solar irradiance variability: Modeling the measurements. *Earth and SpaceScience*, 7, e2019EA000645. <https://doi.org/10.1029/2019EA000645>

Li, X., Wu, T., Liu, K., Li, Y., & Zhang, L. (2016). Evaluation of the Chinese fine spatial resolution hyperspectral satellite TianGong-1 in urban land-cover classification. *Remote Sensing*, 8(5), 438. <https://doi.org/10.3390/rs8050438>

Liberti, G. L., D'Alimonte, D., di Sarra, A., Mazeran, C., Voss, K., Yarbrough, M., et al. (2020). European radiometry buoy and infrastructure (EURYBIA): A contribution to the design of the European Copernicus infrastructure for ocean colour system vicarious calibration. *Remote Sensing*, 12(7), 1178. <https://doi.org/10.3390/rs12071178>

Lin, G., Wolfe, R. E., Dellomo, J. J., Tan, B. & Zhang, P. (2020). SNPP and NOAA-20 VIIRS on-orbit geolocation trending and improvements. In *SPIE Proceedings, Earth Observing Systems XXV*, edited by J. J. Butler, X. Xiong, X. Gu, Proc. SPIE Vol. 11501, 1150112. <https://doi.org/10.1117/12.2569148>

Lin, G., Wolfe, R. E., & Nishihama, M. (2011). NPP VIIRS geometric performance status, In *SPIE Proceedings, Earth Observing Systems XVI*, edited by J. J. Butler, X. Xiong, X. Gu, Proc. of SPIE, Vol. 8153, 81531V. <https://doi.org/10.1117/12.894652>

Lin, G., Wolfe, R. E. & Tilton, J. C. (2016). Trending of SNPP ephemeris and its implications on VIIRS geometric performance. In *SPIE Proceedings, Earth Observing Systems XXI*, edited by J. J. Butler, X. Xiong, X. Gu, Proc. of SPIE Vol. 9972, 99721K. <https://doi.org/10.1117/12.2239043>

Lin, G., Wolfe, R. E., Tilton, J. C., Zhang, P., Dellomo, J. J., & Tan, B. (2018). JPSS-1/NOAA-20 VIIRS early on-orbit geometric performance. In *SPIE Proceedings, Earth Observing Systems XXIII*, edited by J. J. Butler, X. Xiong, X. Gu, Proc. SPIE 10764, 107641H. <https://doi.org/10.1117/12.2320767>

Lin, G., Wolfe, R. E., Zhang, P., Dellomo, J. J., & Tan, B. (2022). Ten years of VIIRS on-orbit geolocation calibration and performance. *Remote Sensing*, 14, 4212. <https://doi.org/10.3390/rs14174212>

Lin, G., Wolfe, R. E., Zhang, P., Tilton, J.C., Dellomo, J.J., & Tan, B. (2019). Thirty-six combined years of MODIS geolocation trending. In *SPIE Proceedings, Earth Observing Systems XXIV*, edited by J. J. Butler, X. Xiong, X. Gu, Proc. SPIE Vol. 11127, 1112715. <https://doi.org/10.1117/12.2529447>

Maiersperger, T. K., Scaramuzza, P. L., Leigh, L., Shrestha, S., Gallo, K. P., Jenkerson, C.B., & Dwyer, J. L. (2013). Characterizing LEDAPS surface reflectance products by comparisons with AERONET, field spectrometer, and MODIS data. *Remote Sensing of Environment*, 136, 1-13. <https://doi.org/10.1016/j.rse.2013.04.007>

Malthus, T. J., Ong, C., Lau, I., Fearn, P., Byrne, G., Thankappan, M., et al. (2019). A community approach to the standardised validation of surface reflectance data. *A Technical Handbook to Support the Collection of Field Reflectance Data. Release version 2.0*, January 2019. CSIRO, Australia. ISBN: 978-1-4863-0991-7

Masek, J. G., Wulder, M. A., Markham, B., McCorkel, J., Crawford, C. J., Storey, J., & Jenstrom, D.T. (2020). Landsat 9: Empowering open science and applications through

continuity. *Remote Sensing of Environment*, 248, 111968.
<https://doi.org/10.1016/j.rse.2020.111968>

Meister, G., Kwiatkowska, E. J., Franz, B. A., Patt, F. S., Feldman, G. C., & McClain, C. R. (2005). Moderate-Resolution Imaging Spectroradiometer ocean color polarization correction. *Applied Optics*, 44(26), 5524-5535. <https://doi.org/10.1364/AO.44.005524>

Micijevic, E., Rengarajan, R., Haque, M.O., Lubke, M., Tuli, F.T.Z., Shaw, J.L., et al. (2022). ECCOE Landsat quarterly calibration and validation report—Quarter 3, 2021: U.S. Geological Survey Open-File Report 2022–1025, 38 p. <https://doi.org/10.3133/ofr20221025>

Montanaro, M., Gerace, A., Lunsford, A., & Reuter, D. (2014). Stray light artifacts in imagery from the Landsat 8 Thermal Infrared Sensor. *Remote Sensing*, 6(11), 10435-10456.
<https://doi.org/10.3390/rs6110435>

Mouroulis, P., & McKerns, M. M. (2000). Pushbroom imaging spectrometer with high spectroscopic data fidelity: Experimental demonstration. *Optical Engineering*, 39, 808.
<https://doi.org/10.1117/1.602431>

Müller, R. (2014). Calibration and verification of remote sensing instruments and observations. *Remote Sensing*, 6(6), 5692-5695. <https://doi.org/10.3390/rs6065692>

National Academies of Sciences, Engineering, and Medicine (2018). *Thriving on Our Changing Planet: A Decadal Strategy for Earth Observation from Space*. Washington, DC: The National Academies Press. <https://doi.org/10.17226/24938>

National Oceanic and Atmospheric Administration Earth System Research Laboratory (1995). *Surface Radiation Budget (SURFRAD) Network Observations*. NOAA National Centers for Environmental Information.

Nicodemus, F. E., Richmond, J. C., Hsia, J. J., Ginsberg, I. W., & Limperis, T. (1977). *Geometrical considerations and nomenclature for reflectance*. Final Report National Bureau of Standards. U.S. Department of Commerce.

Ong, C., Thome, K., Heiden, U., Czaplá-Myers, J., & Mueller, A. (2018). Reflectance-based imaging spectrometer error budget field practicum at the Railroad Valley Test Site, Nevada [Technical Committees]. *IEEE Geoscience and Remote Sensing Magazine*, 6(3), 111-115.
<https://doi.org/10.1109/MGRS.2018.2841934>

Pearlshtien, D. H., Ben-Dor, E. (2022). CalVal evaluation of DESIS products in Amiaz Plain and Makhtesh Ramon test sites, Southern Israel. *The International Archives of Photogrammetry, Remote Sensing and Spatial Information Sciences*, 46, 13-21. <https://doi.org/10.5194/isprs-archives-XLVI-1-W1-2021-13-2022>

Pearlshtien, D. H., Pignatti, S., Greisman-Ran, U., & Ben-Dor, E. (2021). PRISMA sensor evaluation: a case study of mineral mapping performance over Makhtesh Ramon, Israel. *International Journal of Remote Sensing*, 42(15), 5882-5914.
<https://doi.org/10.1080/01431161.2021.1931541>

Pérez Díaz, C. L., Xiong, X., Li, Y., & Chiang, K. (2021). S-NPP VIIRS thermal emissive bands 10-year on-orbit calibration and performance. *Remote Sensing*, 13(19), 3917. <https://doi.org/10.3390/rs13193917>

Pignatti, S., Palombo, A., Pascucci, S., Romano, F., Santini, F., Simoniello, T., et al. (2013). The PRISMA hyperspectral mission: Science activities and opportunities for agriculture and land monitoring. In *2013 IEEE International Geoscience and Remote Sensing Symposium-IGARSS* (pp. 4558-4561). IEEE. <https://doi.org/10.1109/IGARSS.2013.6723850>

Polz, L., Serdyuchenko, A., Lettner, M., Mücke, M., & Fischer, S. (2021). Setups for alignment and on-ground calibration and characterization of the EnMAP hyperspectral imager. *Proceedings of SPIE 11852, International Conference on Space Optics — ICSO 2020*, 118526B. (Vol. 11852, pp. 2583-2596). <https://doi.org/10.1117/12.2600240>

Quattrochi, D. A., & Luvall, J. C. (Eds.). (2004). *Thermal remote sensing in land surface processes*. Boca Raton, Florida. Taylor & Francis Group, CRC Press LLC.

Ramaseri Chandra, S.N., Christopherson, J.B., Casey, K.A., Lawson, J., Sampath, A., (2022). Joint Agency Commercial Imagery Evaluation - Remote sensing satellite compendium: U.S. Geological Survey Circular 1500, 279 p., <https://doi.org/10.3133/cir1500>. [Supersedes USGS Circular 1468]

Rengarajan, R., Sampath, A., Storey, J., & Choate, M. (2015). Validation of geometric accuracy of Global Land Survey (GLS) 2000 data. *Photogrammetric Engineering and Remote Sensing*, 81(2), 131-141. <https://doi.org/10.14358/PERS.81.2.131>

Rengarajan, R.; Storey, J. C.; & Choate, M. J. (2020). Harmonizing the Landsat ground reference with the Sentinel-2 global reference image using space-based bundle adjustment. *Remote Sensing*, 12(19), 2132. <https://doi.org/10.3390/rs12193132>

Richter, R., & Schläpfer, D. (2019). Atmospheric and topographic correction (ATCOR theoretical background document) Version 1.1, March 2021. DLR Report DLR-IB 564-03/2019; German Aerospace Center (DLR): Wessling, Germany, 2019; Available online: https://www.rese-apps.com/pdf/atcor_atbd.pdf (accessed on 31 January 2023).

Roy, D. P., Wulder, M. A., Loveland, T. R., Woodcock, C. E., Allen, R. G., Anderson, M. C., et al. (2014). Landsat-8: Science and product vision for terrestrial global change research. *Remote Sensing of Environment*, 145, 154-172. <https://doi.org/10.1016/j.rse.2014.02.001>

Ruddick, K. (2023), HYPERNET site locations, personal communication.

Salisbury, J. (2022). The Geosynchronous Littoral Imaging and Monitoring Radiometer (GLIMR): NASA's newest ocean color mission. *44th COSPAR Scientific Assembly*. Held 16-24 July, 44, 95.

Schaepman-Strub, G., Schaepman, M. E., Painter, T. H., Dangel, S., & Martonchik, J.V. (2006). Reflectance quantities in optical remote sensing—definitions and case studies, *Remote Sensing of Environment*, 103(1), 27-42. <https://doi.org/10.1016/j.rse.2006.03.002>

Seo, D., Oh, J., Lee, C., Lee, D. & Choi, H. (2016). Geometric calibration and validation of Kompsat-3A AEISS-A camera, *Sensors*, 16(10), 1776. <https://doi.org/10.3390/s16101776>

Shea, Y., Fleming, G., Kopp, G., Lukashin, C., Pilewskie, P., Smith, P., Thome, K., Wielicki, B., Liu, X., Wu, W. (2020). Clarreo Pathfinder: Mission Overview and Current Status, IGARSS 2020 - 2020 IEEE International Geoscience and Remote Sensing Symposium, Waikoloa, HI, USA, pp. 3286-3289. <https://doi.org/10.1109/IGARSS39084.2020.9323176>

Stavros, E. N., Chrono, J., Cawse-Nicholson, K., Freeman, A., Glenn, N. F., Guild, L., et al. (2022). Designing an Observing System to Study the Surface Biology and Geology of the Earth in the 2020s. *Journal of Geophysical Research - Biogeoscience*. <https://doi.org/10.1002/essoar.10509039.1>

Stone, T. C., Coddington, O., Bak, J., & Doelling, D. (2021). Vis/NIR subgroup proposes TSIS-1 HRS as the GSICS recommended solar spectrum. In Ball, M.(Ed.) *GSICS Quarterly Newsletter Spring 2021 Issue*, 15(1).<https://doi.org/10.25923/m6pq-w122>

Stone, T. C., Kieffer, H. H., Lukashin, C., & Turpie, K. (2020). The Moon as a climate-quality radiometric calibration reference. *Remote Sensing*, 12(11), 1837. <https://doi.org/10.3390/rs12111837>

Storch, T., Bachmann, M., Honold, H. P., Kaufmann, H., Krawczyk, H., Müller, R., et al. (2014). EnMAP data product standards. In *2014 IEEE Geoscience and Remote Sensing Symposium* (pp. 2586-2589). IEEE. <https://doi.org/10.1109/IGARSS.2014.6947002>

Storey, J. C., Choate, M., & Lee, K. (2014). Landsat 8 Operational Land Imager on-orbit geometric calibration and performance. *Remote Sensing*, 6(11), 11127–11152. <https://doi.org/10.3390/rs6111127>

Storey, J. C., Rengarajan, R., Choate, & M. J. (2019). Bundle adjustment using space-based triangulation method for improving the Landsat global ground reference. *Remote Sensing*, 11(14), 1640. <https://doi.org/10.3390/rs11141640>

Sun, J., & Xiong, X. (2021). Improved lunar irradiance model using multiyear MODIS lunar observations. *IEEE Transactions on Geoscience and Remote Sensing*, 59(6), 5154–5170. <https://doi.org/10.1109/TGRS.2020.3011831>

Swayze, G. A., Clark, R. N., Goetz, A. F., Livo, K. E., Breit, G. N., Kruse, F. A., & Ashley, R. P. (2014). Mapping advanced argillic alteration at Cuprite, Nevada, using imaging spectroscopy. *Economic Geology*, 109(5), 1179-1221. <https://doi.org/10.2113/econgeo.109.5.1179>

Tansock, J., Bancroft, D., Butler, J. Cao, C., Datla, R., Hansen, S., et al. (2015). *Guidelines for radiometric calibration of electro-optical instruments for remote sensing*, NISTHB 157. Gaithersburg, MD. <https://doi.org/10.6028/NIST.HB.157>

Taylor, S., Adriaensen, S., Toledano, C., Barreto, A., Woolliams, E., & Bouvet, M. (2021). LIME: the Lunar Irradiance Model of the European Space Agency. In EGU General Assembly 2021, online, 30 Apr 2021. <https://doi.org/10.5194/egusphere-egu21-10066>

Thompson, D. R., Brodrick, P. G., Cawse-Nicholson, K., Chadwick, K. D., Green, R. O., Poulter, B., et al. (2021). Spectral fidelity of Earth's terrestrial and aquatic ecosystems. *Journal of Geophysical Research: Biogeosciences*, 126(8): e2021JG006273.
<https://doi.org/10.1029/2021JG006273>

Tilton, J. C., Lin, G., & Tan, B. (2017b). Measurement of the band-to-band registration of the SNPP VIIRS imaging system from on-orbit data, *J. Selected Topics in Applied Earth Observations and Remote Sensing*, 10(3), 1056-1067.
<https://doi.org/10.1109/JSTARS.2016.2601561>

Tilton, J. C., Wolfe, R.E., & Lin, G. (2017a). On-orbit line spread function estimation of the SNPP VIIRS imaging system from Lake Pontchartrain causeway bridge images, *J. Selected Topics in Applied Earth Observations and Remote Sensing*, 10(11), 5056-5072.
<https://doi.org/10.1109/JSTARS.2017.2729879>

Tilton, J. C., Wolfe, R.E., Lin, G., & Dellomo, J.J. (2019). On-orbit measurement of the effective focal length and band-to-band registration of satellite-borne whiskbroom imaging sensors. *Journal of Selected Topics in Applied Earth Observations and Remote Sensing*, 12(11), 4622-4633. <https://doi.org/10.1109/JSTARS.2019.2949677>

USDA (2023). USDA Geospatial Data Gateway, NAIP orthoimage data. Available online: <https://datagateway.nrcs.usda.gov/GDGHHome.aspx> (accessed on 31 January 2023)

USGS (2018). USGS EROS Archive - Aerial Photography - Digital Orthophoto Quadrangle (DOQs). Available online: <https://www.usgs.gov/centers/eros/science/usgs-eros-archive-aerial-photography-digital-orthophoto-quadrangle-dogs#overview> (accessed on 31 January 2023)

USGS (2021). Landsat 8-9 Calibration and Validation (Cal/val) Algorithm Description Document (ADD). Available online: <https://www.usgs.gov/media/files/landsat-8-9-calibration-validation-algorithm-description-document> (accessed on 31 January 2023)

Vane, G., Goetz, A. F., & Wellman, J. B. (1984). Airborne imaging spectrometer: A new tool for remote sensing. *IEEE Transactions on Geoscience and Remote Sensing*, 6, 546-549.
<https://doi.org/10.1109/TGRS.1984.6499168>

Vansteenkoven, D., Ruddick, K., Cattijse, A., Vanhellemont, Q., Beck, M. (2019). The pan-and-tilt hyperspectral radiometer system (PANTHYR) for autonomous satellite validation measurements – prototype design and testing. *Remote Sensing*, 11(11), 1360.
<https://doi.org/10.3390/rs11111360>

Vuppala, H. (2017). Normalization of pseudo-invariant calibration sites for increasing the temporal resolution and long-term trending (Master's thesis) Retrieved from Electronic Theses and Dissertations (<https://openprairie.sdstate.edu/etd/2180>). Brookings, SD: South Dakota State University.

Waluschka, E., McCorkel, J., McIntire, J., Moyer, D., McAndrew, B., Brown, S. W., et al. (2015). VIIRS/J1 polarization narrative. In *Proc. of SPIE, Earth Observing Systems XXII*.
<https://doi.org/10.1117/12.2190138>

- Wan, Z., Zhang, Y., Zhang, Q., & Li, Z.-L. (2002). Validation of the land surface temperature products retrieved from Terra Moderate Resolution Imaging Spectroradiometer data. *Remote Sensing of Environment*, 83, 163-180. [https://doi.org/10.1016/S0034-4257\(02\)00093-7](https://doi.org/10.1016/S0034-4257(02)00093-7)
- Wang, Y., Hu, X., Chen, L., Huang, Y., Li, Z., Wang, S., et al. (2020). Comparison of the lunar models using the hyper-spectral imager observations in Lijiang, China. *Remote Sensing*, 12(11), 1878. <https://doi.org/10.3390/rs12111878>
- Wang, Z., Xiong, X. and & Li, Y. (2015). Update of VIIRS on-orbit spatial parameters characterized with the Moon. *IEEE Transactions on Geoscience and Remote Sensing*, 53(10), 5486-5494. <https://doi.org/10.1109/TGRS.2015.2423633>
- Wang, M., Yang, B., Hu, F., & Zang, X. (2014). On-orbit geometric calibration model and its applications for high-resolution optical satellite imagery. *Remote sensing*, 6(5), 4391-4408. <https://doi.org/10.3390/rs6054391>
- Wenny, B. N., Helder, D., Hong, J., Leigh, L., Thome, K. J. & Reuter, D. (2015). Pre- and post-launch spatial quality of the Landsat 8 Thermal Infrared Sensor, *Remote Sensing*, 7, 1962-1980. <https://doi.org/10.3390/rs70201962>
- Werdell, P. J., Behrenfeld, M. J., Bontempi, P. S., Boss, E., Cairns, B., Davis, G. T., et al. (2019). The Plankton, Aerosol, Cloud, ocean Ecosystem mission: Status, science, advances. *Bulletin of the American Meteorological Society*, 100(9), 1775-1794. <https://doi.org/10.1175/BAMS-D-18-0056.1>
- Wielicki, B. A., Doelling, D. R., Young, D. F., Loeb, N. G., Garber, D. P., & MacDonnell, D. G. (2008). Climate quality broadband and narrowband solar reflected radiance calibration between sensors in orbit. *IGARSS 2008 - 2008 IEEE International Geoscience and Remote Sensing Symposium*, I-257-I-260. <https://doi.org/10.1109/IGARSS.2008.4778842>
- Wilkens, L., Sang, B., Erhard, M., Bittner, H., Grzesik, A., Eberle, S., et al. (2017). An on-board calibration assembly (OBCA) on the EnMAP satellite. In *International Conference on Space Optics—ICSO 2016* (Vol. 10562, p. 1056244). International Society for Optics and Photonics. <https://doi.org/10.1117/12.2296123>
- Woodward, J. T., Turpie, K. R., Stone, T. C., Gadsden, S. A., Newton, A., Maxwell, S. E., et al. (2022). Measurements of absolute, SI-traceable lunar irradiance with the airborne lunar spectral irradiance (air-LUSI) instrument. *Metrologia*, 59, 034001. <https://doi.org/10.1088/1681-7575/ac64dc>
- Xiong, X., Angal, A., Chang, T., Chiang, K., Lei, N., Li, Y., et al. (2020). MODIS and VIIRS calibration and characterization in support of producing long-term high-quality data products. *Remote Sensing*, 12(19), 3167. <https://doi.org/10.3390/rs12193167>
- Xiong, X., Angal, A., Sun, J., Choi, T., & Johnson, E. (2014). On-orbit performance of MODIS solar diffuser stability monitor. *Journal of Applied Remote Sensing*, 8(1), 083514-083514. <https://doi.org/10.1117/1.JRS.8.083514>

Xiong, X., Wenny, B. N., Wu, A., Barnes, W. L., & Salomonson, V. V. (2009). Aqua MODIS thermal emissive band on-orbit calibration, characterization, and performance. *IEEE Transactions on Geoscience and Remote Sensing*, 47(3), 803-814.
<https://doi.org/10.1109/TGRS.2008.2005109>

Zandbergen, S. R., Mouroulis, P., Small, Z., Bender, H. A., & Bellardo, J. (2020). Snow and water imaging spectrometer: Final instrument characterization. In *Imaging Spectrometry XXIV: Applications, Sensors, and Processing* (Vol. 11504, pp. 27-39). SPIE.
<https://doi.org/10.1117/12.2569144>

Zibordi, G., & Mélin, F. (2017). An evaluation of marine regions relevant for ocean color system vicarious calibration. *Remote sensing of environment*, 190, 122-136.

Zibordi, G., Melin, F., Berthon, J.-F., Holben, B., Slutsker, I., Giles, D., et al. (2009). AERONET-OC: A network for the validation of ocean color primary products. *Journal of Atmospheric and Oceanic Technology*, 26(8), 1634-1651.
<https://doi.org/10.1175/2009JTECHO654.1>

Zong, Y., Brown, S.W., Johnson, B. C., Lykke, K. R., & Ohno, Y. (2006). Simple spectral stray light correction method for array spectroradiometers. *Applied Optics*, 45, 1111.
<https://doi.org/10.1364/AO.45.001111>

Appendix A - Acronyms used in this paper.

There are many acronyms used throughout this paper. They are listed here for easy reference.

AERONET, AErosol RObotic NETwork

AERONET-OC, AERONET - Ocean Color, a network of stations with upward and downward pointed instruments for measuring water-leaving reflectances.

air-LUSI Mission, airborne LUNar Spectral Irradiance Mission

AIS, Airborne Imaging Spectrometer

AOP, apparent optical properties

ARD, Analysis Ready Data

ASR, absolute spectral response

AVIRIS, Airborne Visible / InfraRed Imaging Spectrometer

AVIRIS-NG, AVIRIS Next Generation

BBR, band-to-band registration

BOUSSOLE, Buoy for the acquisition of long-term optical time series

BRDF, Bi-Directional Reflectance Distribution Function

Cal/Val, Calibration and Validation

CE90, circular error at the 90th percentile

CEOS, Committee on Earth Observation Satellites

CHIME, Copernicus Hyperspectral Imaging Mission for the Environment

CHRIS, Compact High Resolution Imaging Spectrometer

CLARREO, Climate Absolute Radiance and Refractivity Observatory

CNES, Centre National d'Etudes Spatiales (The French Space Agency)

CPF, CLARREO-Pathfinder

CVWG, Calibration and Validation Working Group (of the SBG Mission)

DEM, Digital Elevation Model

DEGIS, German Aerospace Center (DLR, Deutsches Zentrum für Luft- und Raumfahrt) Earth Sensing Imaging Spectrometer

DO, Designated Observable

DOQ, digital orthophoto quadrangles

ECOSTRESS, ECOsystem Spaceborne Thermal Radiometer Experiment on Space Station

ECV, Essential Climate Variables

EGM, Earth Gravitational Model

EMIT, Earth Surface Mineral Dust Source Investigation

EnMAP, Environmental Mapping and Analysis Program

EOC, early orbit check-out

EPICS, extended PICS

ESA, European Space Agency

ESAS, Earth Science and Application from Space

ESO, Earth System Observatory

EURYBIA, European Radiometry Buoy and Infrastructure

FLARE, Field, Line-of-sight Automated Radiance Exposure

FLEX, FLuorescence EXplorer mission

FWHM, full width at half maximum

GCP, Ground Control Point

GIRO. GSICS Implementation of the ROLO model

GLAMR, Goddard Laser for Absolute Measurement of Radiance

GLIMR, Geostationary Littoral Imaging and Monitoring Radiometer

GLS, Global Land Survey

GPS, The Global Positioning System

GRI, Global Reference Image

GSD, ground sampling distance

GSFC, Goddard Space Flight Center

GSICS, Global Space-based Inter-Calibration System

HISUI, Hyperspectral Imager Suite

HSRS, Hybrid Solar Reference Spectrum of TSIS-1

HyMap, an airborne hyperspectral sensor

HypIRI, Hyperspectral Infrared Imager

HYPERNET-EU, federated network of automated hyperspectral radiometers on zenith- and azimuth- pointing systems deployed on fixed structures for satellite validation, combining LANDHYPERNET and WATERHYPERNET. The project is managed by the Royal Belgian Institute for the Natural Sciences.

ICV, intensive calibration and validation

IEEE, Institute of Electrical and Electronics Engineers

IFOV, instantaneous field of view

IOP, inherent optical properties

ISO, International Organization for Standardization

ISRO, Indian Space Research Organisation

ISS, International Space Station

LANDHYPERNET, federated network of automated hyperspectral radiometers on zenith- and azimuth- pointing systems deployed on fixed structures, providing land reflectance data for satellite validation. The project is managed by the Royal Belgian Institute for the Natural Sciences.

LIME, Lunar Irradiance Model ESA

L_{max}, Maximum radiance that can be measured by a radiometric instrument.

L_{min}, Minimum radiance that can be measured by a radiometric instrument.

LOPA, Loss of pointing accuracy

L_{sat}, Radiance at which a sensor saturates

LTAN, Local Time Ascending Node

LTDN, Local Time Descending Node

LSTM, Land Surface Temperature Monitoring

MarONet, Marine Optical Network

MOBY, Marine Optical BuoY

MODIS, MODerate resolution Imaging Spectroradiometer

MODTRAN, MODerate resolution atmospheric TRANsmission

MSI, Multi-Spectral Instrument

MTF, modulation transfer function

NAIP, National Agriculture Imagery Program of the USDA

NASA, National Aeronautics and Space Administration

NASEM, National Academies of Science, Engineering and Medicine

NET, No earlier than

NFR, Near Field Response

NIR, Near-infrared

NOAA, National Oceanic and Atmospheric Administration

NSO, near-simultaneous nadir observations

OCI, Ocean Color Instrument (of PACE)

OLI, Operational Land Imager

OOB, out-of-band

OSSE, Observing System Simulation Experiments

PACE, Phytoplankton Aerosols Clouds and ocean Ecology

PICS, pseudo invariant calibration sites

PRISMA, PRecursores IperSpettrale della Missione Applicativa (Hyperspectral Precursor of the Application Mission)

PROBA, Project for On-Board Autonomy, (ESA technology demonstration missions)

PTFE, Polytetrafluoroethylene

QVD, Quartz Volume Diffuser

RadCalNet, Radiometric Calibration Network

RadCaTS, Radiometric Calibration Test Site

ROLO, Robotic Lunar Observatory

RSR, relative spectral response

SATM, Science and Applications Traceability Matrix

SBG, Surface Biology and Geology

SeaPRISM, SeaWiFS Photometer Revision for Incident Surface Measurements

SeaWiFS, Sea-viewing Wide Field-of-view Sensor

SDSM, Solar Diffuser Stability Monitors

SHALOM, Space-borne Hyperspectral Applicative Land and Ocean Mission

SI, International System of Units

SIRCUS, Spectral irradiance and radiance responsivity calibrations using uniform sources

SNO, simultaneous nadir observation

SRF, spectral response function

SSO, Sun-synchronous orbit

SURFRAD, Surface Radiation Budget Network

SVC, system vicarious calibration

T-SIRCUS, Traveling SIRCUS

TIR, thermal infrared

TOA, top-of-atmosphere

TRISHNA, Thermal infraRed Imaging Satellite for High-resolution Natural resource Assessment

TSIS, Total Solar Irradiance Sensor (US NASA)

T/Vac, Thermal/Vacuum chamber

USDA, US Department of Agriculture

USGS, US Geological Survey

UMBC, University of Maryland, Baltimore County

UVB, ultraviolet B-rays

VIIRS, Visible Infrared Imaging Radiometer Suite

VSWIR, visible-to-shortwave infrared

WATERHYPERNET, federated network of automated hyperspectral radiometers on zenith- and azimuth- pointing systems deployed on fixed structures, providing water reflectance data for satellite validation. The project is managed by the Royal Belgian Institute for the Natural Sciences.

WGCV, Working Group on Calibration and Validation of CEOS